

Advances in deployable structures and surfaces for large apertures in space

J. Santiago-Prowald · H. Baier

Received: 17 May 2013 / Revised: 11 July 2013 / Accepted: 4 August 2013 / Published online: 30 September 2013
© CEAS 2013

Abstract Large apertures in space have applications for telecommunications, Earth observation and scientific missions. This paper reviews advances in mechanical architectures and technologies for large deployable apertures for space antennas and telescopes. Two complementary approaches are described to address this challenge: the deployment of structures based on quasi-rigid members and highly flexible structures. Regarding the first approach, deployable articulated structures are classified in terms of their kinematics as 3D or planar linkages in multiple variants, resulting in different architectures of radial, peripheral or modular constructions. A dedicated discussion on the number of degrees of freedom and constraints addresses the deployment reliability and thermo-elastic stability of large elastic structures in the presence of thermal gradients. This aspect has been identified as a design driver for new developments of peripheral ring and modular structures. Meanwhile, other design drivers are maintained, such as the optimization of mass and stiffness, overall accuracy and stability, and pragmatic aspects including controlled industrial development and a commitment to operators' needs. Furthermore, reflecting surface technologies and concepts are addressed with a view to the future, presenting advances in technical solutions for increasing apertures and reducing areal mass densities to affordable levels for future missions. Highly flexible materials capable of producing ultra-stable shells are

described with reference to the state of the art and new developments. These concepts may enable large deployable surfaces for antennas and telescopes, as well as innovative optical concepts such as photon sieves. Shape adjustment and shape control of these surfaces are described in terms of available technologies and future needs, particularly for the reconfiguration of telecommunications antennas. In summary, the two complementary approaches described and reviewed cover the domain of present and foreseeable space applications. Recent European developments are discussed within a global context and a critical review of the state of the art and recent advances taking into account the reliability and structural stability as design drivers.

Keywords Deployable structures · Structural mechanisms · Overconstrained linkages · Large deployable antennas · Large reflectors · Conical ring structure · Photon sieve · Highly flexible structures · Shell-membrane · Shape memory polymer · Reconfigurable antennas

1 Introduction

Future space missions will require large deployable reflectors (LDR) for telecommunications and specific science and Earth observation applications. In the case of communications satellites, such reflectors with projected apertures typically in the 5–8 m range will have to operate in C-Ku bands for Fixed and Broadcasting Satellite Services (FSS/BSS) and Ku-Ka bands for Broadband Satellite Services. Larger reflectors of up to 25 m projected aperture are already operational, mainly in the L and S bands for Mobile Satellite Services. Other applications include air

J. Santiago-Prowald (✉)
Mechanical Department, European Space Agency, ESTEC,
Keplerlaan 1, Noordwijk, The Netherlands
e-mail: julian.santiago.prowald@esa.int

H. Baier
Institute of Lightweight Structures, Technische Universität
München, 85747 Garching, Germany

traffic management satellite services in L band, as well as emergency and tactical communications systems in VHF/UHF. These and other applications are further detailed in the extensive reviews of space communications mission scenarios and antenna architectures by Mangenot et al. [1] and Amyotte et al. [2].

In Earth observation applications, especially Synthetic Aperture Radar (SAR) in L, C and X bands, reflector-based concepts compete with phased arrays. Although electrical beam shaping and steering capabilities offer a high degree of flexibility to fulfill user requirements, array antenna architectures are typically heavy and the realization of bandwidth and full polarimetric capability introduce additional complexity into the design. Concepts based on a large parabolic reflector antenna offer several advantages. Among them, antenna efficiency, bandwidth, mass, power consumption, complexity and cost can be more controllable [3]. The realization of a fully polarimetric system and broad bandwidths (for a high spatial resolution) are not as difficult and costly as with a direct radiating array antenna. Reflector-based SAR would also enable multi-frequency instruments. Limitations are swath width and beam steering. In L band, interferometric SAR systems have been proposed assuming a bi-static configuration of two or more satellites whereby a master instrument with full SAR capability is accompanied by a slave, and the baseline between the satellites is maintained for a portion of the orbit providing a bi-static interferometric SAR. Large deployable reflector antennas over 15-m aperture have been identified as having potential for such L-band missions. Meanwhile, the BIOMASS mission [4] has been selected by ESA as an Earth Explorer Core Mission. The primary objective of the mission is to estimate forest biomass by means of P-band (435 MHz) SAR observations of global forest cover. This mission requires a reflector with an aperture of 12 m. In addition to SAR, radiometry has also been identified as a potential user of these large apertures. Resolution requirements physically dictate the instrument sensor and, therefore, the antenna sizing, with particular impact on the lower frequency bands.

Taking into account the requirements of telecommunications, Earth observation and radio-astronomy, the functional requirements on the antennas can be divided into two main groups in terms of projected aperture [1]. In the first group, a projected aperture of 4–7 m with an RMS surface accuracy around $\lambda/50$ (i.e. 2.5 mm in S band) for applications mostly in L and S bands or $\lambda/50$ to $\lambda/100$ for applications from C to Ka band (i.e. 0.1 mm in Ka band) is required. The second group corresponds to projected apertures in the range of 9–25 m with an RMS surface accuracy around $\lambda/50$ for applications mostly in UHF and L/S bands. Higher operational frequencies can be required for particular cases such as radiometry and radioastronomy. The pointing stability of the

reflector assembly including the deployable arm should be in the range of 0.01° – 0.1° half cone. Concerning mass, the technology state of the art is around 1 kg/m^2 for the very large apertures; meanwhile for the higher accuracies 2 – 5 kg/m^2 are often the case. The required stiffness is closely related to the AOCS disturbances and spacecraft station-keeping and re-pointing operations [5].

Astrophysics missions need deployable structures mostly for the creation of long base lines of interferometers and large focal lengths, e.g., for X-ray telescopes. Missions currently in early phases require for instance deployable booms of up to 100 m deployed length and positioning accuracy within a sphere of 1 mm radius or better and rotations lower than 0.005 degree. An extensive review has been performed by Puig et al. [6]. Large deployable apertures on the other hand would obviously provide increased sensitivity and angular resolution to telescopes, although current technologies offer only the solution of hinged mirror segments vis-à-vis the required shape accuracy, as in the RadioAstron and James Webb Space Telescope. This is still an open field for deployable or highly flexible structures incorporating other solutions with higher structural efficiency.

Concerning available technologies, deployable structures in space have enabled a range of applications and performances which are not possible otherwise. Classical examples are foldable solar arrays providing a very large planar surface for the collection of solar radiation. In the case of antennas, the proportionality of antenna directivity to surface area is also a driver, although the surface is typically a parabolic reflector. In all cases the problem at hand is the efficient packaging and mass reduction of a structure that results in a large aperture with sufficient stiffness and stability when deployed. Two classical approaches have been employed for the mechanical architecture since the start of space activities: the folding of rigid members at discrete joints by means of devoted mechanisms and the elastic deformation of structures, allowing a transition from folded to deployed states by the controlled release of strain energy. Both architectures are in fact complementary; the two methods can be combined in hybrid constructions of rigid and elastic members. The fact that pre-tension may be applied at the end of the deployment can be an additional design driver. However, the main selection criteria for space applications are mass and stiffness, stowed package dimensions, stability and deployment reliability. As discussed in [1], surface accuracy can be very demanding, especially in the aperture range up to 5 m for the higher RF bands. Nevertheless, this requirement determines the reflecting surface material and supporting elements design. For the deployable structure, the surface accuracy requirement translates into stability and stiffness of the structure.

Fig. 1 MBB unfurlable mesh reflector during deployment testing (courtesy of EADS Astrium and ESA)



The historical background of deployable antennas in the European context is remarkable, although it cannot be said to be a success story so far. The first programmes intended for flight hardware were initiated by ESA in the early 1980s with the Contraves' 12-m inflatable reflector and the 5-m aperture Unfurlable Mesh Antenna developed by MBB (see Fig. 1). The latter is in essence a hinged-rib antenna architecture. The industrial developments were discontinued in spite of the incipient commercial interest at the time, leaving the field free for other products to capture the telecommunications and institutional markets.

Another example of European discontinued investments is the ERA 9-m antenna (Fig. 2) by Aerospaziale, now Astrium-ST. It is based on a truss of deployable triangular prism elements supporting a metal mesh. It was flown in 1988 on the MIR station.

Pantograph ring concepts and associated technologies have been conceived and developed since the early 1980s for the Soviet space programmes, originating at the Georgian Technical University (GTU), Institute for Space Constructions [7, 8]. The ring architecture consisting of a 5.5-m aperture peripheral pantograph structure with radially tensed membrane ribs was flown and deployed on the MIR station in 1999 (Fig. 3). This architecture and the development team contributed significantly to ESA's 12 m large deployable antenna (LDA) development, within the ARTES programme (Fig. 4).

To date, the LDA has been the only space programme to implement a deployable pantograph ring in an industrial context. The ground qualification phase of a 12-m aperture antenna was achieved under ESA contract with Thales Alenia Space of Italy as prime contractor and NPO-EGS, a joint venture between GTU and Korolev RSC Energia of Moscow, as reflector provider [9] (see Fig. 4). Despite some technical difficulties, the qualification programme showed compliance with the requirements, and the aspects of the design that required improvement were identified.

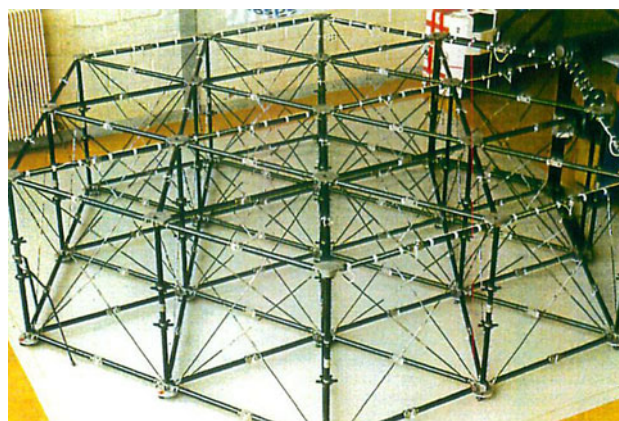


Fig. 2 Structure deployment test of the Aerospaziale ERA 9 m antenna (Courtesy Astrium-ST)

Once more, the development did not find its way to a flight qualification and product development, in part due to the complexity of the industrial organization.

The LDA programme was the latest attempt to provide a European large antenna product. This concept and the previous ones shown above are now considered obsolete and would require major improvements to produce a competitive product. Therefore, following the conclusions of the ESA Large Antenna Working Group (LAWG), established across several directorates, it has been recommended that new developments should be initiated to correct the current absence of a European reflector antenna product with a projected aperture larger than 4 m. In this direction, the Large Antenna Workshop, which took place at ESTEC on 2–3 October 2012, presented the technological advances, endorsing the LAWG recommended activities [1].

This paper summarizes some of these activities within a review of general concepts and the state of the art in deployable structures for space. The reader is referred to the workshop proceeding to gain a complete picture. The

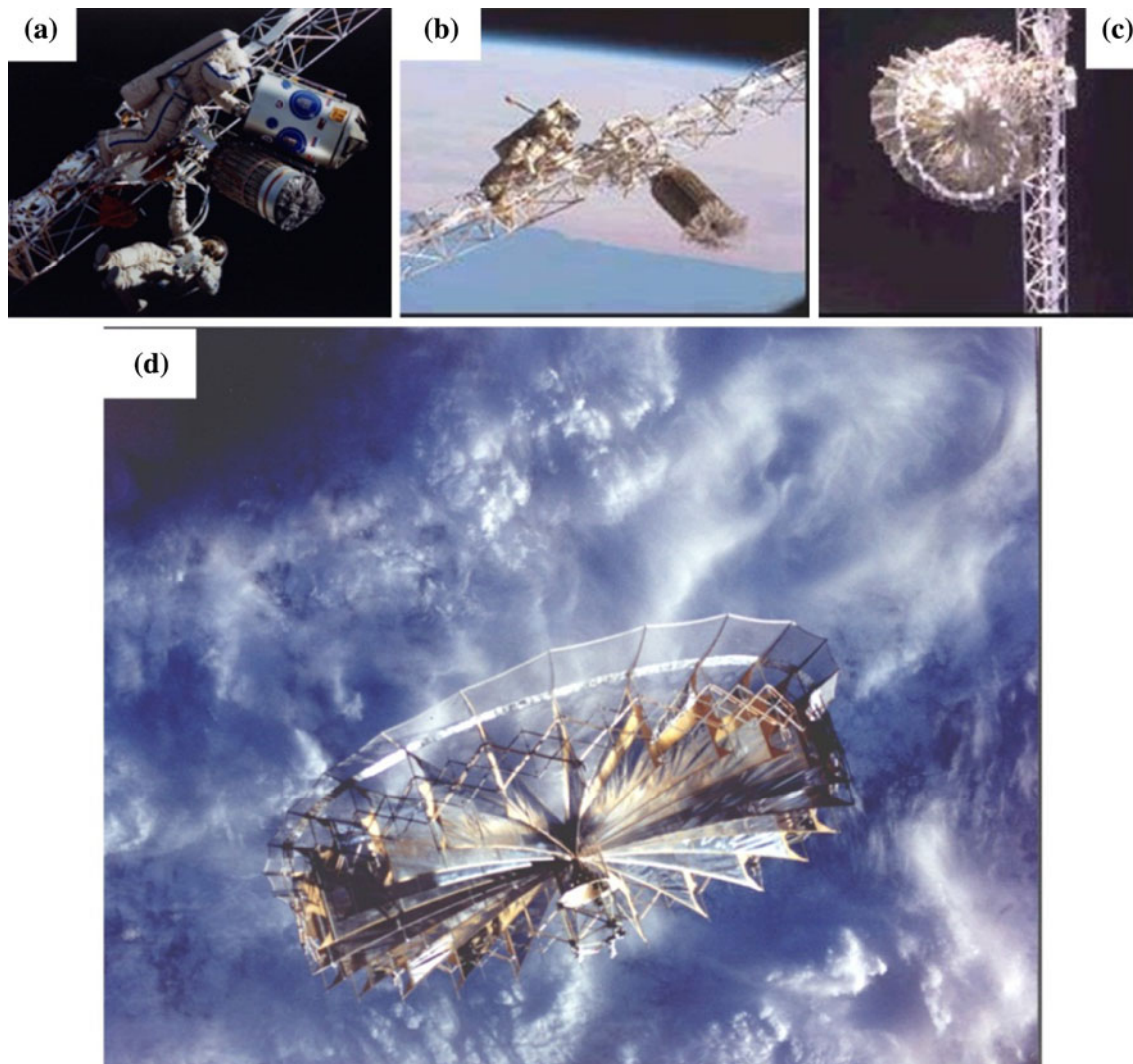


Fig. 3 In-orbit deployment test of the 5.5 m Georgian Mesh Reflector (a, b) stowed on the MIR station (c) deployment, (d) deployed, after separation from the MIR station (Courtesy of GTU)

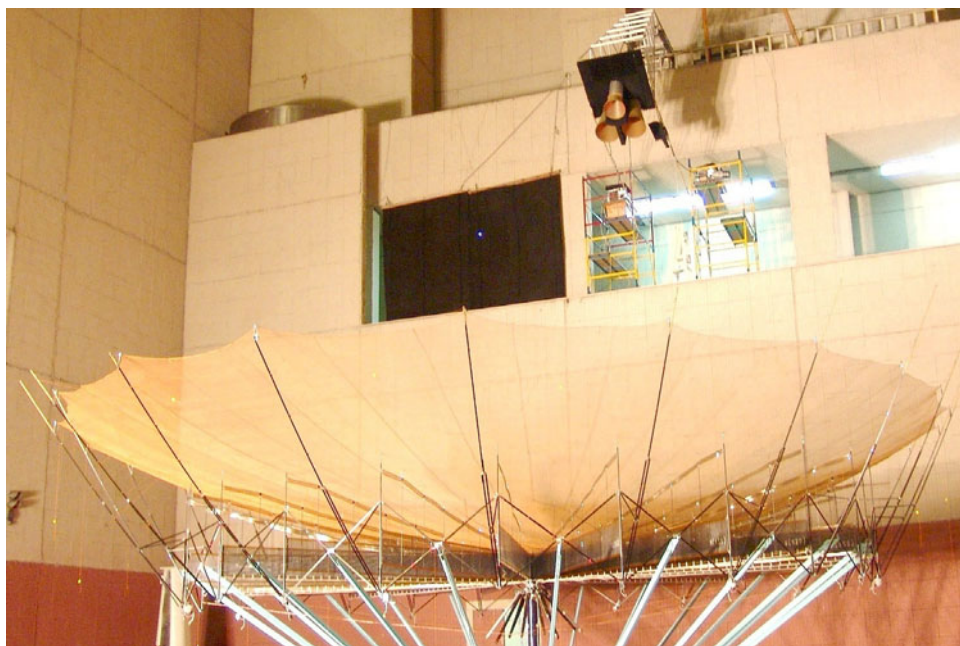
paper is organized into two parts. The first part is devoted to the review of deployable structures from the point of view of kinematics. The deployment mechanisms are classified as planar and three-dimensional and the different types and variants are discussed in view of their characteristics with respect to deployable reflectors. Special emphasis is given to the understanding of mobility and degrees of freedom and the importance of their control and robustness. Also in the first part, highly flexible structures are briefly discussed. Further deepening on highly elastic structures is provided in Sect. 3 in the context of reflecting surfaces. Several types of surfaces are described, including the classical metal knitted meshes and the recently developed shell-membranes. This section also addresses the possible future developments of large telescopes in the direction of higher structural efficiency and the associated technologies. Section 4 provides an introduction to the

shape adjustment and control of surfaces by implementation of shape memory materials and piezo-electric polymers. Section 5 addresses a particular application of shell-membranes to reflector reconfiguration for telecommunications.

2 Advances in deployable structures architectures

This section provides an overview of two distinct and complementary approaches for creating large deployable structures in space for large apertures: the deployment of structures made of quasi-rigid members connected by kinematic pairs, and highly flexible structures that deploy by the controlled release of strain energy or by inflation. The focus will be placed on the former type, also referred to as structural mechanisms, by classifying the existing

Fig. 4 Large deployable antenna EQM in deployed configuration (Courtesy of TAS-I, NPO-EGS and ESA)



deployment schemes as planar and spatial. This kinematic classification refers to the unit cell that is repeated in peripheral rings, radial arms or as a spatial module for building double-curvature surfaces. Most of these unit cells are made of bar linkages with revolute and cylindrical joints. The actuation can be provided by electrical motors or elastic elements. From the discussion, it will be concluded that one of the key aspects is the determination of the degrees of freedom during the deployment phases, to control the trajectories without bifurcation, instability, jamming or collision, as well as the thermo-elastic stability in the deployed state.

Deployable mesh reflectors, the largest group of LDR, have been built for space applications following different construction schemes. The majority of them can be classified topologically as *radial* (e.g., Lockheed's Wrap-Rib antenna, the Japanese HALCA antenna for VLBI, Harris' Rigid-Rib and Hinged-Rib, ESA's MBB antenna, ISS-Reshetnev's Lutch antennas), *peripheral* (e.g., Northrop-Grumman's AstroMesh, Harris' hoop-truss and hoop-column, GTU's MIR reflector experiment, ESA's LDA) or *modular* structures (e.g., JAXA's ETSVIII, OKB-MEI's TKSA-6, Tashkent's KRT10) [1, 10–12]. In the case of radial structures, the reflecting surface is less supported at the edges, meanwhile in the peripheral ring case, the centre region is unsupported. Thus, in both topologies, auxiliary means of shape control and tensioning devices are required. This limitation is mitigated when the structure is a collection of distributed and kinematically coupled modules. The price of this latter approach is probably the higher complexity and reduced reliability. Obviously, intermediate solutions are also possible. Actually, the JAXA modular

antenna consists of modules of a significant size, which can be used already as radial deployable reflectors themselves, especially the Tri-Fold antenna [13]. The classification of structures presented hereafter is not based on existing products or the topological differences as in previous studies. An analysis of the deployment schemes from the point of view of the kinematics has been followed instead. This approach allows a deeper understanding and a synthesis of the new concepts to be presented more thoroughly.

Reflectors constructed by articulation of solid panels are not studied hereafter in detail, due to the fact that their kinematics can be considered as a particular case of the general principles analyzed. Furthermore, these are often unique developments for very particular missions with demanding shape accuracy and RF reflectivity requirements, such as RadioAstron [14]. Further discussion is provided in [1, 10].

2.1 Overview of 3D bar linkages for space deployable structures

Overconstrained spatial nR bar linkage mechanisms (bars linked by revolute joints with $n \geq 4$) represent a particular type of closed-chain mechanisms with interesting properties for large deployable space structures. These overconstrained linkages have deserved special attention since the identification of the first mechanism of this type by Sarrus in 1853 [15], a particular spatial single mobility 6-bar linkage (see Fig. 5). The overconstrained nature of some linkage mechanisms with respect to Grübler–Kutzbach criterion can be considered as a consequence of particular geometries in the kinematic chains of bars connected by rotational pairs, simply reflecting the complexity of 3D chains comprising a

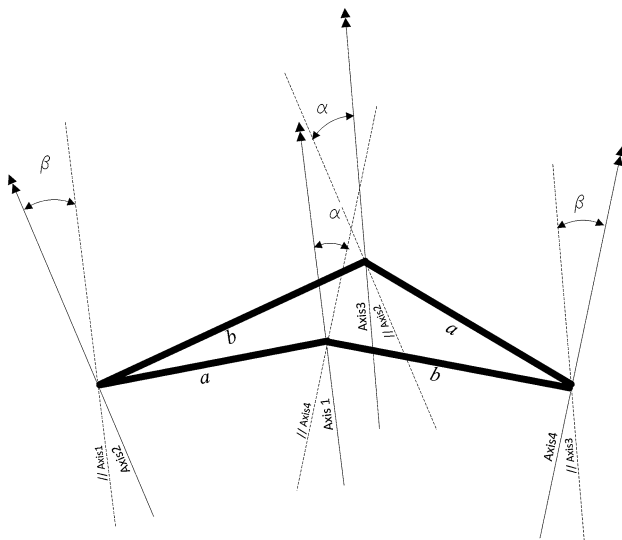


Fig. 5 Classical examples of overconstrained spatial bar linkages with only revolute joints exhibiting single mobility: Bennett skew isogram (*left*) and Sarrus 6-bar linkage (*right*)

large number of elements. According to the mobility criterion applied to 3D bar linkages with only revolute joints, the minimum number of bars for a single degree of freedom is seven. However, it has been found that four bars can be connected by four revolute joints ($4R$) in this way under certain conditions, as in Bennett's skew isogram [16], sketched in Fig. 5. This apparent conundrum has not inhibited the discovery of complex linkages with single mobility; on the contrary, the creativity of designers seems to have been spurred by this fact. A systematic review of spatial overconstrained linkages with a historical perspective has been recently published by Chen and You [17], as a follow on of the classical publications of Baker [18]. There are a limited number of known possibilities for spatial $4R$, $5R$ and $6R$ overconstrained mechanisms. So far, Bennett's loop is the only spatial $4R$ mechanism known and serves as basis for higher order chains.

Spatial five-bar linkages with revolute joints are mainly the Goldberg $5R$ and Myard linkages (see e.g., [19]). Goldberg $5R$ linkages [20] can be obtained by combining a pair of Bennett linkages either by summation or subtraction. Myard [21] produced the first known overconstrained $5R$ linkage, which exhibits plane-symmetry and can be considered as a particular case of the Goldberg $5R$ linkage.

$6R$ linkages are more common and hence several types have been synthesized over the years, starting with Sarrus. Among the $6R$ linkages are the well-known Bricard loops, which can be classified into six variants, one of them giving, e.g., the famous *kaleidocycle* (a ring of at least 6 hinged tetrahedra that can turn in a continuous motion). There are more $6R$ overconstrained bar linkages identified [17], but in general it can be concluded that the Bennett and

Bricard loops are the basic building blocks from which most of the higher order overconstrained linkages can be derived [18].

This family of mechanisms has implications in various scientific disciplines, such as crystallography and materials science, in addition to pure mechanics. The positive feature offered by these mechanisms to machine engineering is that the overconstrained nature, if well controlled, provides additional load paths and enhanced stiffness. This is actually a benefit for industrial applications as in the case of the *Turbula* mixer and potentially also for machine-tool heads and robotics, as it can provide stable positioning. However, these features have to be well controlled in aerospace applications where mass, thermo-elastic stability and reliability are the design drivers in addition to stiffness. Overconstraining could lead to non-compliance and jamming during the deployment process or to unwanted thermo-elastic distortions in a space environment. For those reasons, desmodromic mechanisms and isostatic structures are typically preferred by designers. In addition, the spatial character of the motion is not always optimal for packaging or controlling the spatial envelopes and interferences with other spacecraft elements, which turn out to be often the most demanding requirements.

A classic example of space application of the Sarrus loop within a longitudinal deployable structure can be identified in the well-known FAST mast, used for the deployment of the solar arrays on the International Space Station [11]. Recent developments in deployable antenna structures based on overconstrained 3D linkages have been carried out using the Sarrus loop as a building block [22]. The alternative constructions explored by the authors include a Sarrus 6-bar linkage as the facets of a peripheral ring, although the final design is a hybrid Sarrus loop in which one of the linkages is replaced by a pantograph scissor pair. This architecture is also overconstrained, although it can be controlled by detailed study of tolerances, distortions and failure modes. In both cases, a conical ring is considered for exploiting the stiffening effect provided as compared to a cylindrical ring.

The Myard linkage has been recently integrated successfully into a deployable antenna structure [23], showing that a spatial network of Myard linkages can be obtained starting with the combination of triple Myard loops into a cell. The overall structure made of such cells has still single mobility. Other combinations of Myard linkages allow building hexagonal constructions among other possibilities. The concept has been subject to optimization of mass and stiffness, resulting in an attractive solution.

The spatial overconstrained mechanisms with single mobility discussed so far are kinematically different from most of the flown modular structures made by combination of deployable tetrahedra, prisms or hexahedra. Several

examples of these are already well known, such as the 5-m structure consisting of tetrahedra linked in a hexagonal assembly, developed by Surrey University [24, 25] with the support of British Aerospace. Other examples are the modular antennas developed in Tashkent or the TKSA-5 and TKSA-6 antennas built by OKB-MEI of Moscow, which are trusses of foldable tetrahedra as the basic element. The deployment reliability of modular topologies is governed by the relative synchronization, the matching of the modules and the distribution of resistance and actuation. Typically, the actuation of these structures is through springs distributed over the whole structure in large numbers. See Fig. 6, where some undeployed linkages can be observed.

Another example is the ERA 9-m antenna of Aerospatiale (Fig. 2), a truss of deployable triangular prism elements. The deployment of each element involves the transformation of facets of 12 articulated elements (6 struts in a V-folding parallelogram and another 6 articulated rods as stiffening diagonals). Even if the truss was successfully tested and flight demonstrated on-board the MIR station, the complexity and flexibility of the design for covering the parameters and requirements of large antennas were questioned.

All these spatial constructions require a careful analysis of the degrees of freedom and actuation during deployment and stability in deployed configuration, to avoid possible singularities, loss of control during deployment or excessive thermal distortions when deployed. These analyses can be particularly complex considering the actuation principle, the number of members and the complexity of the joints.

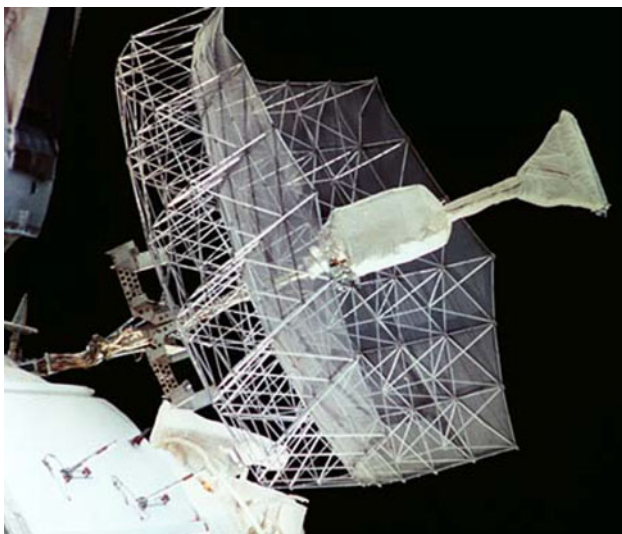


Fig. 6 TKSA-6 antenna on the Priroda Module of the MIR station, flown in 1995, developed by OKB-MEI of Moscow

Tensegrity structures have been proposed for deployable space antennas [26, 27]. These structures are characterized by internally pre-stressed and free-standing networks, in which continuous cables are tensioned against a system of struts in compression. The challenge is given by the form-finding process, especially during deployment, even more complex than the deployment analysis of bar linkages. If considered for the deployable structure as a peripheral ring, the stowed package dimensions are compromised by the necessary lengths of the bars to maintain the system tensioned. Furthermore, it is deemed particularly difficult to demonstrate reliability during deployment and the handling of single point failure modes. The concept can be, however, of interest when considering the architecture of interior regions of peripheral rings, as has been successfully implemented in civil engineering. Well-known examples are the Zalewski, Fuller or Geiger tension domes (e.g., the impressive Seoul Olympic gymnastics stadium of 120 m and the Amagi dome). See [28] for a thorough discussion of the state of the art. Application of these concepts to antenna surfaces has been first proposed by Medzmariashvili and later by Comet Ingenieria, although not yet implemented.

2.2 Overview of planar bar linkages for space deployable antenna structures

Most of the structural mechanisms developed and flown in space within LDAs are in fact based on 2D bar linkages, either in open or closed chains. These linkages remain planar during the deployment or folding, which is a key feature for understanding and controlling complex deployments. The open kinematic chains employed are mainly articulated arms that can be mounted on radial constructions resembling umbrellas. Among these, the most successful reflectors flown so far are the ones developed and manufactured by Harris Corporation of Florida, namely the rigid-rib and hinged-rib antennas. More than 30 reflectors of this kind in the aperture range of 5–18 m are reported to be deployed on-orbit for commercial and TDRS missions [1, 10]. A particular challenge for this architecture is the reflecting mesh management, which requires a large amount of control points, cable networks and special stiffening devices near the edges to provide the required aperture size and shape accuracy. The aspect of reflecting surface shape generation, which is as important as the concept of the structure deployment itself, is treated in the next section.

This category of radial structures includes also the HALCA (MUSES-B) antenna, a realization of the tension truss concept [29, 30]. The reflector has an effective aperture diameter of 8 m. It was built by MELCO for the Institute of Space and Astronautical Science (ISAS). Six

extensible articulated truss masts deploy radially the tension truss network and knitted mesh. Another example is the 5-m aperture Unfurlable Mesh Antenna developed by MBB for ESA in the 1980s (Fig. 1) which in essence has the hinged-rib antenna architecture.

In the case of closed chains, the bar linkages constitute sectors, i.e. facets of a polygonal ring or segments of a mast as mentioned above. One of the reasons of their extensive use as compared to the spatial overconstrained linkages is the predictable behavior and higher reliability. Starting with the four-bar linkage, the most common transformation principles of $4R$ planar bar linkages are the parallelogram of variable diagonal lengths, the pantograph and the triangle with a V-folding bar. See Fig. 7 for sketches of the folding methods. An articulated parallelogram can be moved, e.g., by retracting a cable or by telescopic sliding tubes activated by the cable, as in the case of the Astro-Mesh reflector ring [31, 32], or other actuation principles.

The richness of the classification and the number of possibilities increase by including the actuation principle as a fundamental part of the design, as well as the synchronization between cells. In relation to this topic, the pantograph offers the added advantage of self-synchronization and hence the propagation of the motion from cell to cell. This property has been exploited extensively in 2D and 3D pantographic structures. Several pantograph ring concepts and associated technologies have been deeply developed since the early 1980s for the Soviet space programmes, originating at the Georgian Technical University, Institute for Space Constructions [7]. Among the various types of LDR developed, the ring architecture consisting of a peripheral pantograph structure with radial tensed membrane ribs was flown and deployed on the MIR station in 1999 [8]. In this particular 5.5-m aperture model the double pantograph was implemented by shifting longitudinally in the hoop direction. In doing so the stiffness of the ring was enhanced, although the mass efficiency was not required as the main design driver. Variants and alternative designs were built in the diameter range of 12–30 m, but never flown. Figure 8 shows a picture of the 30-m model during ground testing. It is based on a combination of the single pantograph with V-folding bars coupled at the extremes of the vertical rods, creating an overconstrained 8-bar linkage per facet. See Fig. 7 for a representation of the kinematics. It was driven by long spindle screws.

Other architectures of pantographs and derived linkages have been extensively investigated at GTU [33]. Furthermore, in addition to the Georgian Technical University (GTU) and the Technical University of Munich (TUM), other research groups have investigated pantographic structures. In the University of Cambridge, there has been significant interest in developing masts and double rings based on pantographs as in the Deployable Mesh Reflector

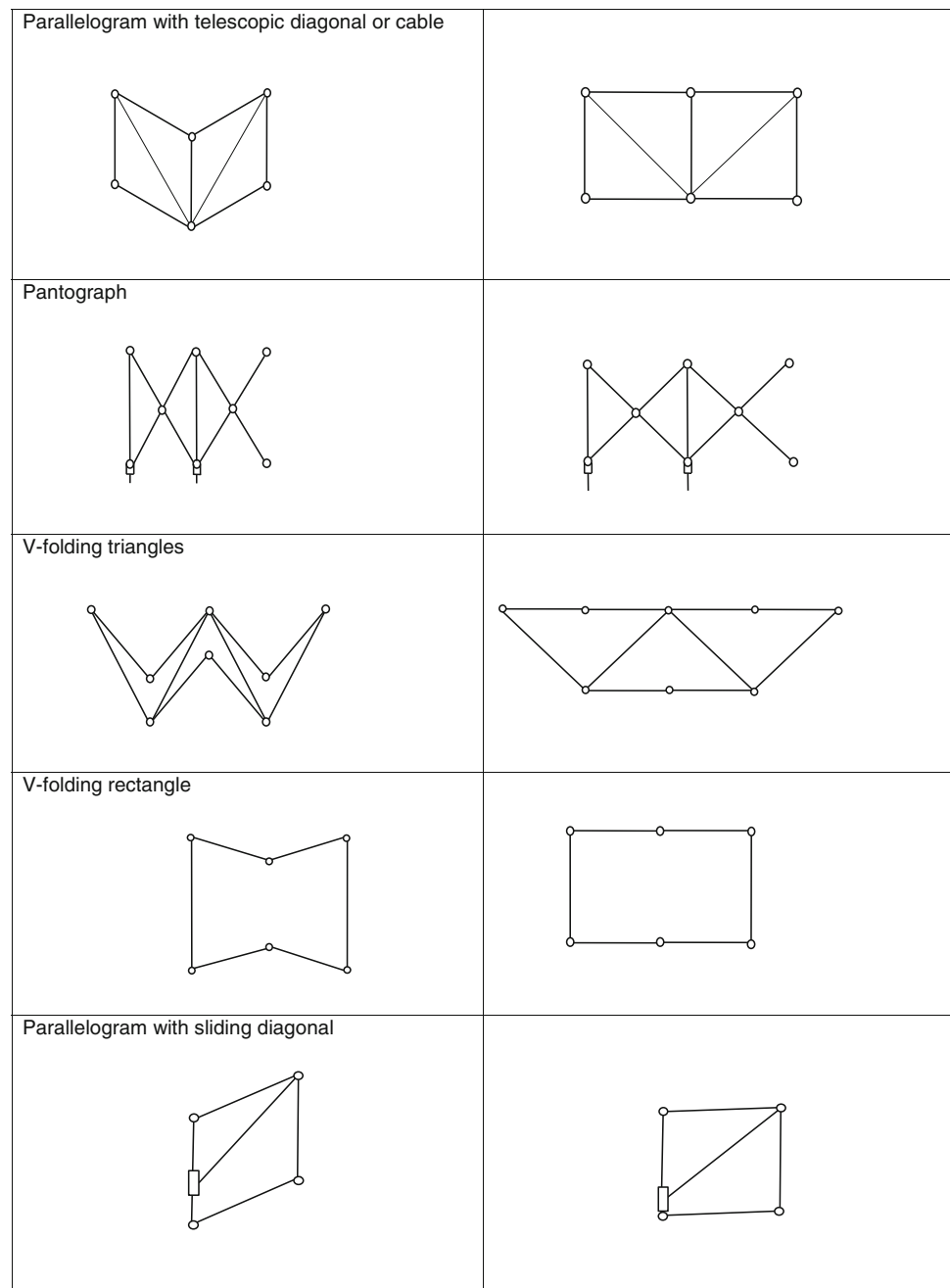
design [25, 34]. The ring structure of this reflector, developed and tested between 1993 and 1994 and described by the authors as an alternative construction of the Harris hoop-column architecture [35] and the Tension Truss Antenna of Miura and Miyazaki [29], is actually a double-pantograph ring. Two peripheral and concentric pantograph rings of different heights are connected radially by a third set of pantograph pairs that adapt to the differing dimensions. In spite of the apparent complexity, the overall mechanism has single mobility and good stiffness and accuracy.

Up to date, ESA's LDA under ARTES contract has been the only space programme within an industrial context implementing a deployable pantograph ring. The ground qualification phase of a 12-m aperture antenna was achieved under ESA contract with Thales Alenia Space of Italy as prime contractor and NPO-EGS, a joint venture of GTU and Korolev RSC Energia of Moscow, as reflector provider. The concept of the ring structure relied on a single circular pantograph equipped with radial articulated extensions. These additional rods, nicknamed 'consoles' by the Russian team, produced the 15 by 12 m elliptical aperture starting from the 10-m ring. To a large extent the design followed the architecture of the MIR antenna experiment of GTU. In this case, the structure was a full carbon-composite articulated truss with radial carbon-composite tape ribs rolled around a central cylinder when stowed [9] (see Fig. 4). The mass of the whole reflector was 57 kg overall. However, despite fulfilling the requirements, the design was criticized for the ring stability and the shape accuracy outside the 10-m circle, mainly due to the consoles deformations [36, 37].

The evolution of the designs towards significantly lighter and more compact stowed package, while maintaining stability and deployment reliability, has led to new variants like the double pantograph shifted vertically, instead of the tangential or radial directions. This has been the topic of developments within 2012 by TUM in collaboration with GTU [38, 39]. A 6-m double separated pantograph demonstrator has been built and functionally tested showing good deployment stability and reliability, in addition to significantly better stowage ratios, a mass of about 10 kg including the actuators and a first eigenfrequency higher than 1 Hz (see Fig. 9). A further variation and relevant characteristic introduced in this design is the crossing of the shifted pantographs while folding, which allows reducing the height of the package to almost the half [39] as compared to the non-crossing pantographs. This demonstrator also includes simplified cable networks similar to the tension truss developed by Miura [29], consisting of triangular networks.

Higher order non-pantographic linkages of 5 or 6 bars connected by revolute and cylindrical joints have also been employed successfully. One of the basic five-bar linkages

Fig. 7 Folding schemes of deployable bar linkages connected by rotational and cylindrical kinematic pairs. Adapted and extended from [7]

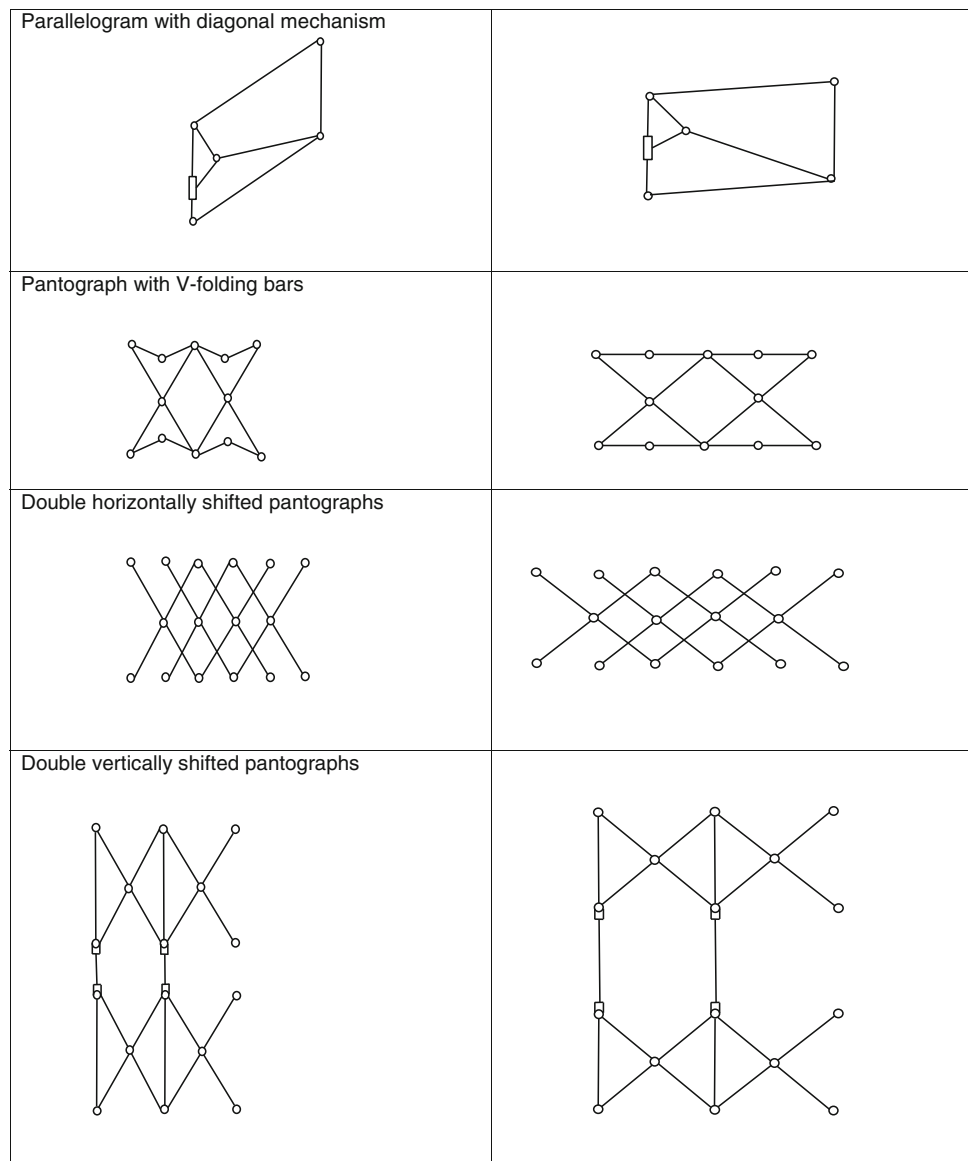


with single mobility and employing a slider is shown in Fig. 7. This apparently simple concept helps to introduce the kinematic description of the foldable arms in the hexagonal module of the NTT modular architecture [40]. One of the designs is a 7-bar linkage, also shown schematically in Fig. 7 for comparison, which served as the basis for the modules of the JAXA 13-m antenna flown on-board ETS-VIII [13, 41]. Even if it is similar to the parallelogram with an extending diagonal, it entails additional elements for providing the motion of the inclined bar with sufficient actuation margin. The linking of three of these parallelograms in a radial arm

has been used in the Trifold configuration, which allows increasing the size of the module significantly [13].

A majority of the mechanisms described above, both in the spatial and planar cases, are in fact overconstrained according to the Grübler–Kutzbach criterion, while still exhibiting a single degree of freedom. This is the case of the parallelogram, tetrahedra or pantograph unitary cells discussed so far, due to the fact that the co-aligned hinges axes introduce redundant constraints in the 3D space. In general applications, this is not a major problem, except when extreme thermal environments may create thermal

Fig. 7 continued



distortions resulting in kinematic incompatibility or the large dimensions and compliances may result in geometrical deviations and misalignments. The risks involved are the jamming of the deployment or the loss of thermoelastic stability. Unfortunately, both are problems that have occurred in well-known space programmes [1], resulting in mission loss or significant reduction of spacecraft performances or mission output. One of the first known examples is the failure of the radial-rib HGA of the Galileo space probe in 1991 [42], although unfortunately very recent cases can be mentioned as well in telecommunications programmes. For these reasons, a controlled implementation of additional kinematic degrees of freedom can be considered key in relation to robustness and reliability, as long as the deployment trajectories

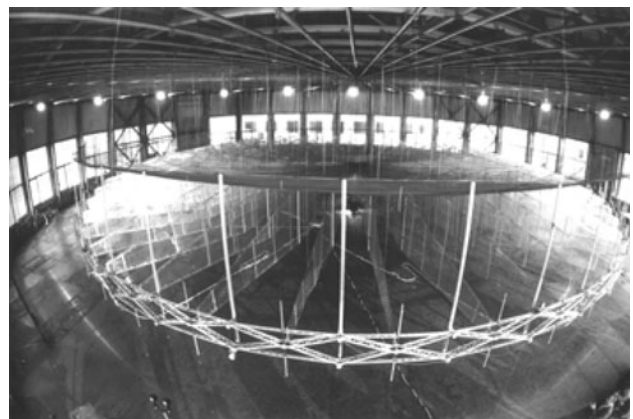


Fig. 8 The 30 m ground demonstration model in the Saguramo complex near Tbilisi (Courtesy of GTU)

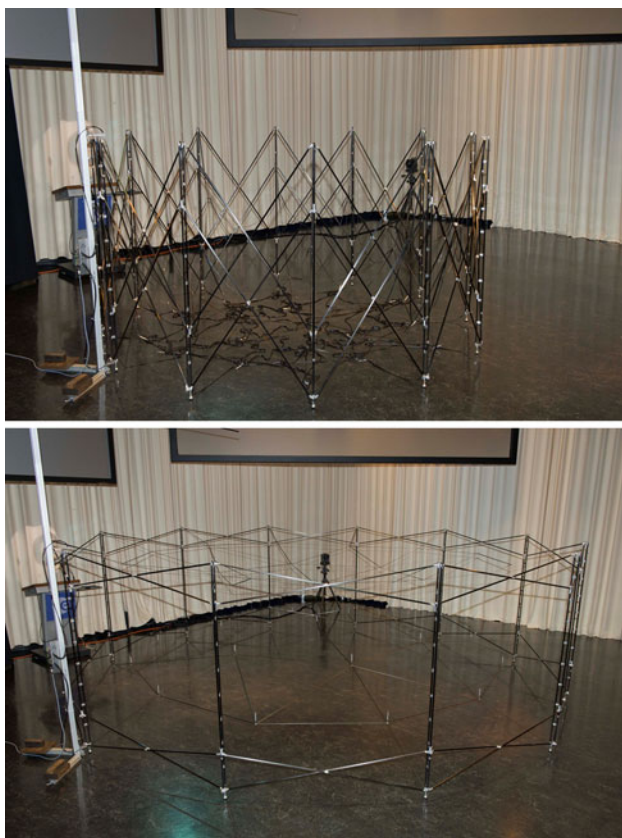


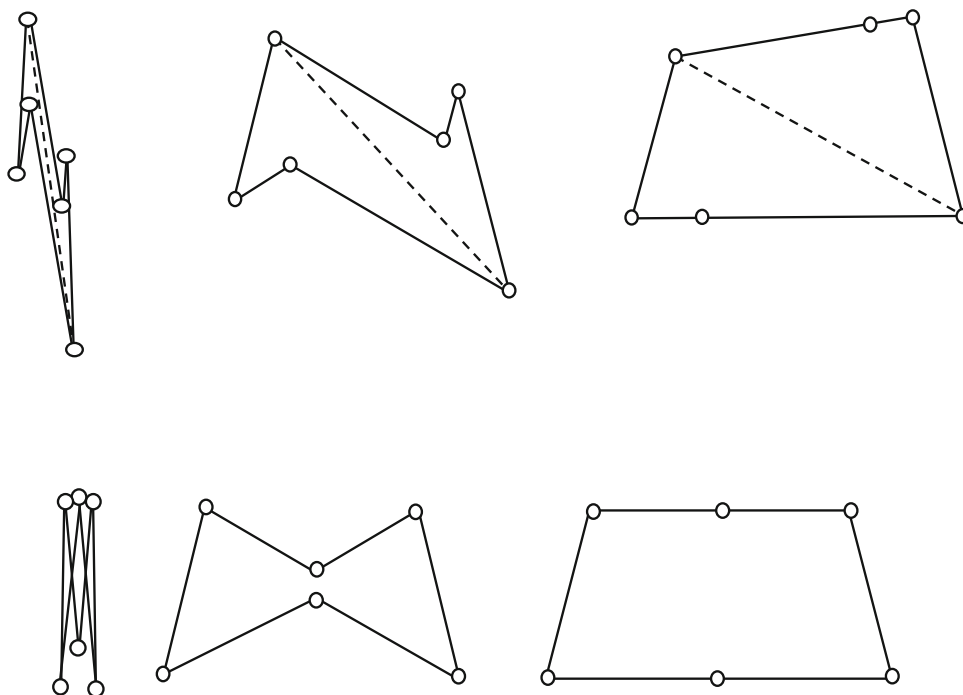
Fig. 9 Deployment test of the 6 m double pantograph ring demonstrator of TUM [39] at ESTEC (Photos ESA/A. Le Floc'h)

remain under control and the potential bifurcations are known and avoided.

Following these ideas, a new type of 6-bar linkage has been proposed, which incorporates potentially more than one degree of freedom while deploying and is fully constrained when deployed [43]. The 6-bar linkage concept is shown in Fig. 10 in the general case of the asymmetric quadrilateral with an optional diagonal stabilizing bar and the particular case of the trapeze (referring to the deployed shape). It employs V-folding bars that reduce the mobility of the linkage when fully extended and provide an advantageous tip-force actuation while deploying. Furthermore, it is based on revolute joints only; therefore, no cylindrical pairs or sliding elements are necessary, which are considered as a potential single point failure.

By integration of several facets in a ring, the 3 planar degrees of freedom of this 6-bar linkage are reduced and controlled due to the synchronization of neighboring facets and the closure of the ring. In addition, the V-fold hinges are actuated and a release control device is implemented. Several options are proposed by Medzmariashvili et al. [44]. The reason of the trapezoidal shape is the fact that a truncated pyramidal or conical construction is obtained by connecting facets. Even in the single ring module case, the deployed structure acquires higher stiffness than in the case of a parallelogram and in addition it can be connected in a modular assembly following the double curvature of parabolic reflectors. Therefore, the planar 6-bar linkage facet defined by this geometry can be used in peripheral rings,

Fig. 10 New 6-bar linkage facet versions implementing higher mobility [43]



longitudinal masts or within modules of a spatial modular construction. Unlike the case of the JAXA antenna, where each module is a hexagon with radial ribs, these modules can be built as peripheral rings in the shape of truncated hexagonal pyramids or any other desired shape. The case of a hexagonal pyramidal module is shown in Fig. 11.

To be able to connect ring modules tiling a double-curvature shape such as the paraboloid, it is necessary to follow certain rules concerning the inclination angle of the facets. These angles depend on the size and number of the modules. One of the possibilities is to design the folding scheme such that the trajectories of the lateral bars follow radial transformations with a common centre. Meanwhile, a further degree of freedom is necessary for transforming the pyramid angle to zero in the folded configuration, i.e. the cylindrical bundle of bars. This requires that the dihedral angle between facets has to be free to rotate within a short range by means of swivels [43, 44]. Two examples are shown in Fig. 12 combining hexagonal modules, although other modules shapes are also possible, including tetrahedral and hexahedral truncated pyramids, regular or irregular. This means that in fact any module polygonal shape can be generated and any surface can be accurately tiled. This strategy could enable very large apertures, estimated in 50 m, in a more efficient way than using radial modules, due to the lower number of folding facets in the overall structure.

A 6-m conical ring with V-folds and electric actuation has been built by GTU and TUM in Tbilisi and functionally tested within 2012 showing good deployment stability and reliability. It has been constructed with the same geometrical parameters as the double-pantograph ring, resulting in a mass of about 10 kg including the actuators and a first eigenfrequency significantly higher than 1 Hz (see Fig. 13). The detailed design is provided by [44]. This demonstrator also includes simplified cable networks similar to the tension truss developed by Miura [29], consisting of asymmetric isostatic triangular networks presented by Rodrigues [45].

On the other hand, the double-pantograph conical ring represents a further development of the pantograph

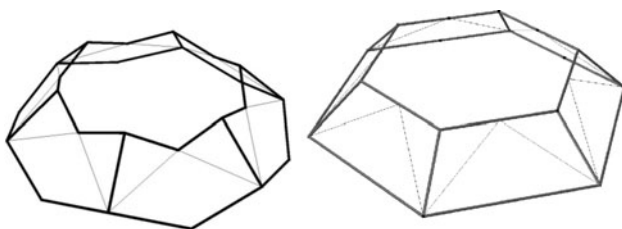


Fig. 11 Hexagonal pyramidal module based on V-folds [43]. Folding scheme alternative as compared to Fig. 10. Release cable routing shown

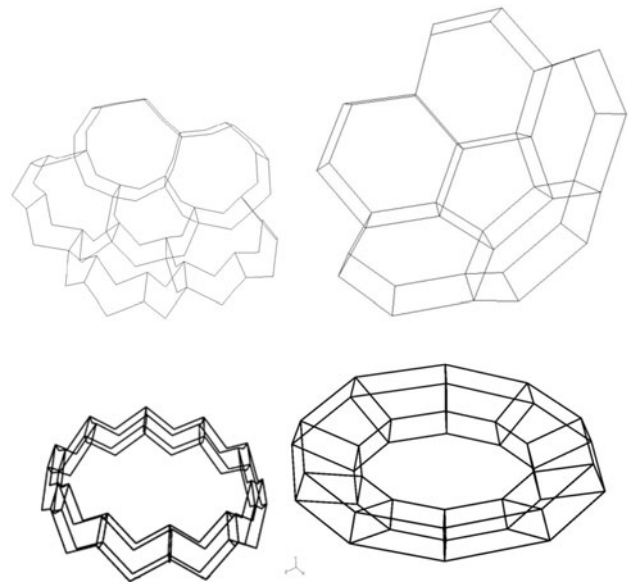


Fig. 12 Possible combinations of hexagonal or rectangular pyramidal modules [43]

architecture [46] incorporating the geometry implemented in the conical construction with V-folds, but now applied to the pantograph. The potential advantage offered by this design is a stiffness increase and self-synchronization, although the stowed package is slightly longer than in the case of V-folds (even if crossing pantographs are considered) and there are some intrinsic over-constraints in spite of the single mobility, as for the cylindrical design. In this case the scissor hinges of one of the pantographs require additional degrees of freedom as compared to the revolute joint [46] (see Fig. 14). In this way, the folding into a cylindrical package is allowed, even if the deployed shape is conical, following a smooth, reversible and kinematically compatible transition. To some extent it can be seen as a recovery of the single mobility when compared to the V-folding, although both designs can be seen as very similar in terms of overall construction.

With the double-pantograph conical ring it would be also possible to generate modular constructions as the ones in Fig. 12. Due to the features described above, both the V-folding conical ring and the double-pantograph ring have been preselected by European industry as the architectures to explore for future developments of LDAs [47, 48]. The main reasons mentioned are the increased compactness of the stowed packages offered by these two concepts, which was taken in fact as one of the main design drivers.

2.3 Highly flexible and hybrid deployable apertures

Highly Flexible Structures represent a wide discipline, covered in numerous papers and books. They include

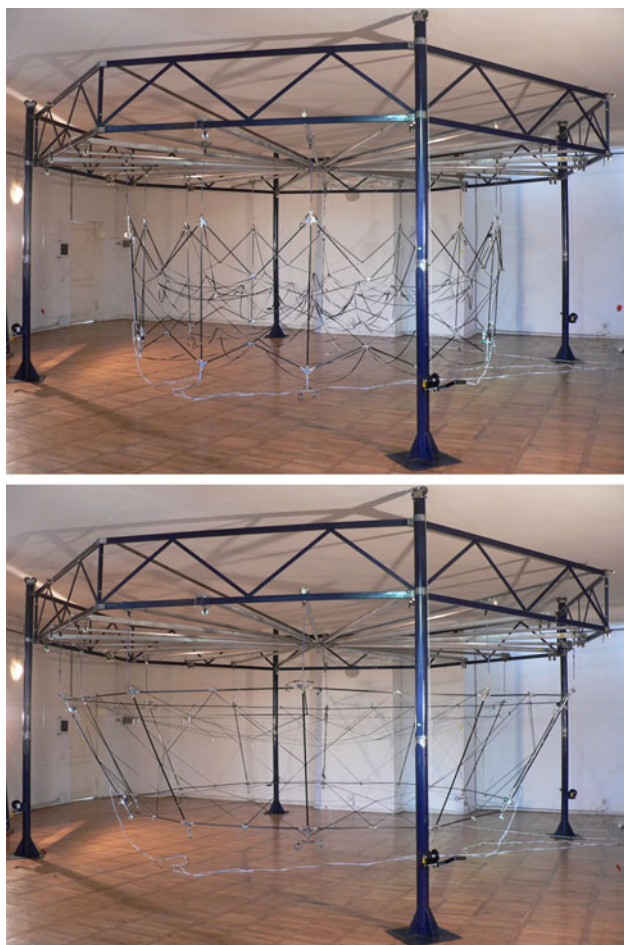


Fig. 13 Deployment test of 6 m conical ring demonstrator of GTU/TUM/ESA [44] at GTU in Tbilisi

inflatable structures made of very thin membranes, mechanisms-free deployable structures submitted to large elastic deformation, exploiting snap-through, local buckling, self-locking and other non-linear phenomena for stowage and deployment. The full extent of the discipline lies beyond the scope of this review; only a general overview is provided and some relevant examples listed. A summary of representative cases of highly flexible structures, their space applications and characteristics are addressed succinctly by Pellegrino [11], including among other the coilable mast, the Collapsible Tube Mast, prestressed membranes and inflatable structures. The extensive work of Frank Pai [49] is proposed as a relevant reference for the design, analysis and testing methods. In Sect. 3, the topic is further discussed for the generation of reflecting surfaces.

The challenge for highly flexible structures in space applications, apart from the size and mass efficiency, resides in the verification approach [50]. This is due to the fact that from the system engineering perspective a total predictability and control of their degrees of freedom during their life are required, especially during the in-orbit

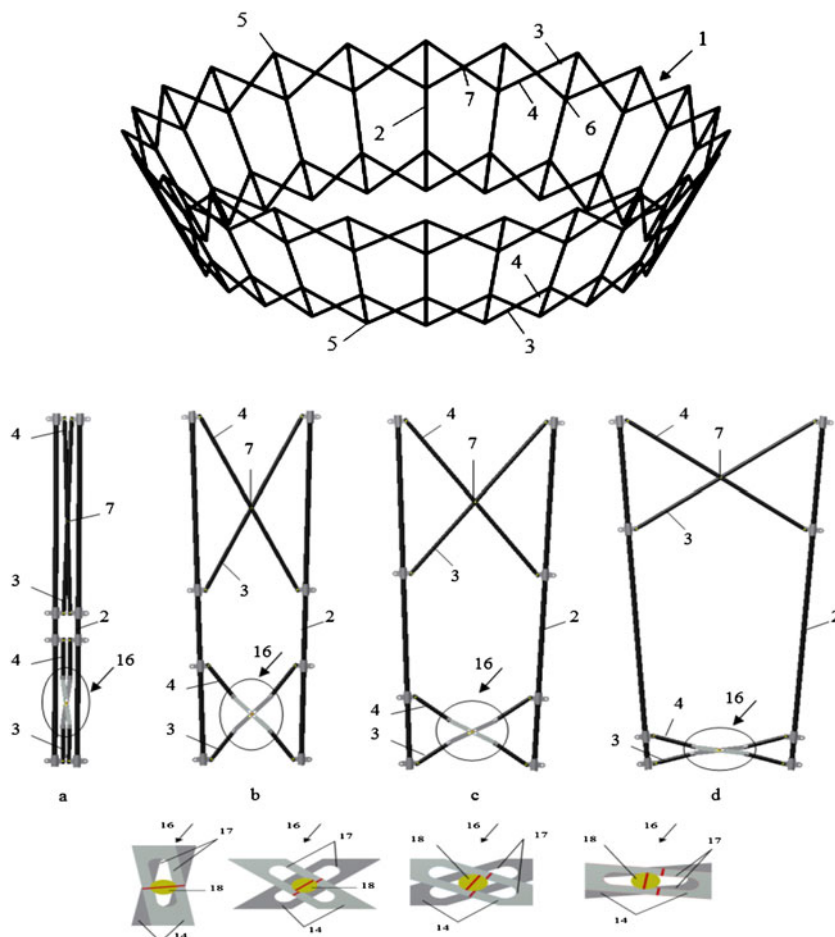
deployment phase. In addition, their scalability laws depend on combinations of many parameters and environmental conditions, which results in complex and costly qualification programmes. Very often, the system issues are ultimately linked to very detailed aspects of material properties, such as creep, thermal sensitivity, vacuum compatibility and physicochemical degradation under radiation and meteoroid environments [51].

The simplest of these elements are cables, which are normally treated as mostly inextensible, but highly flexible in bending and not capable of sustaining compression. This results in the fact that they have to be always submitted to tension to make their motion predictable. A loose cable is in fact a potential failure in space. Hence, it is evident that already one of the simplest highly flexible elements is submitted to constraints and exhibits uncertainty from the system engineering point of view. Even more challenging is the controlled release of elastically folded beams, plates, membranes and shells, for which the number of degrees of freedom is simply not countable and the preload can represent a danger to neighboring equipment. Therefore, the task consists in their controlled release. On the other hand, the knowledge and control of elastic folding elements and the resulting structures can represent a very valuable asset.

Several antenna reflectors have been developed using the principles of highly flexible shells and membranes [1]. Among them are the Spring Back reflectors, developed by Hughes and flown onboard several TDRS missions. Further studies have been performed by the University of Cambridge and University College London, resulting in the stiffened spring-back concept [52, 53]. These studies involved a deep optimization of the reinforcement ribs and edge skirts. By these modifications, most of the strain energy and deformation are localized in spring-like elements integrated in the structure. Folding capabilities have been exploited to the extreme at TUM by Datashvili and Baier with the development of the CFRS, silicone matrix composite reinforced with triax or biax carbon fabrics. The material exhibits interesting properties, developed and deeply studied within the TAHARA and SAFIRS activities under ESA contracts [53, 54].

A particular example of hybrid construction, integrating localized elasticity and rigid bodies, is the concept of elastic hinges without kinematic pairs or discrete actuators. From the system point of view, this is an attractive solution since the controllability of the deployment is largely improved as compared to the fully flexible option [55, 56]. The key point is in the detailed understanding of internal stresses and failure modes in the micro-scale, while establishing the relationships to the macro-scale degrees of freedom. This is the main direction of the research at this point in time, driven by University of Cambridge and more recently by Caltech. The remaining open issues are: end-of-

Fig. 14 Double pantograph conical ring architecture and scissor joint detail [46].
Courtesy of GTU/TUM/ESA



deployment shock emission and material creep in the stowed state. These seem to remain as open points although intense work is being carried out. Nevertheless, the state of the art is such that from systems point of view, a discrete hinge mechanism with elastic or electric actuation is normally baselined.

3 Deploying reflecting surfaces

This section is devoted to address recent advances in reflecting surfaces for LDR and their applications, with additional remarks also on future large deployable telescopes. Proper concept definitions for telecommunications, Earth observation and possibly also astronomy require a good synthesis between RF or optical considerations and the mechanical reflector and reflective surface aspects.

Related requirements pose high challenges to LDRs. Responses to such challenges are mainly in:

- Precision deployment and related topics;
- Accurate reflecting surfaces;

- Dimensionally stable materials and structures;
- Possibilities of shape adjustment and control.

The technologies have to be combined with proper analysis, manufacturing and integration approaches. Testing also puts new challenges due to the size and resulting high elastic flexibility of the reflector in deployed configuration. Gravity load effects on the reflecting shape might be considerable with considerable effort needed for sufficient compensation for on-ground verification.

In addition to such considerations on the “passive” mechanical concepts and materials, active means such as shape control may further improve the LDR’s performance especially for applications in short wavelengths. In shape control, shape deviations due to disturbances are to be compensated to the best possible extent by actuators triggered by control signals such that the reflector’s shape is as close as possible to the ideal one. In contrast to this, shape morphing reflectors, also known as reconfigurable reflectors, have to *change* their shape during their mission in orbit sometimes to adapt to new mission needs. Since this may require quite high morphing amplitudes and spatial frequencies, proper design and material concepts

together with shape morphing actuation have to be established then.

This overview suggests that concept definitions should be preferably based on building blocks allowing the selection of reflecting surfaces out of different types and to combine it with proper deploying and stiffening structures. While for the latter, the focus was given in the previous section, emphasis in the following will be more on reflecting surfaces and materials.

To highlight the state of the art, reference is taken to the general literature, with an intentional bias on different investigations and activities done within ESA studies and which are only partly addressed in the other papers of this edition of the Journal. After a brief overview on different reflecting surface technologies, specific aspects of membranes and meshes are addressed, followed by those related to shell-membranes mostly composed from carbon fiber reinforced silicone (CFRS). Shape control will be briefly addressed mostly as a quasi-static problem, with some side considerations on possible micro-vibrations or jitter effects and their attenuation. Some remarks on possible transfer of these technologies to future deployable large telescopes are also given. Mechanically reconfiguring or shape morphing reflectors will be also briefly addressed. The discussions will be concluded by an outlook also on further technology needs.

3.1 Reflecting surfaces criteria and concepts overview

Promising approaches to satisfy the above-mentioned needs are concepts based on ultra-stable membranes and very thin shells, sometimes also inflatable and space rigidizing. Such structures and reflecting surfaces are part of the family of Gossamer structures, with an overview on these given by Salama and Jenkins [57]. Membranes might be also generated by tensioned meshes approaching the ideally required, e.g., parabolic surface by a large set of planar surfaces. It is obvious that in case of required high surface accuracy, then a high number of very small planar facets would then have to be generated. In contrast to this, the so-called shell-membranes directly aim for achieving double curved shapes and by this avoid the planar approximation error. They have quite low bending stiffness just large enough to achieve double curvature in orbit but are flexible enough to be stowable nearly like membranes. Such shell-membranes are composed of certain C-fiber topologies integrated into special flexible “rubber type” space proven silicone matrix materials. The resulting composite is called CFRS. It is the small thickness together with this flexible matrix which provides low flexibility to stow and sufficient stiffness to achieve double curved shape once deployed. Such meshes, membranes and shell-membrane reflecting surfaces then are used in combination with

highly precise deployment and stiffening structures mainly made out of CFRP, as discussed in previous sections.

In addition to proper deployment and shape accuracy and stability, scalability and technological growth potential as well as a certain robustness are further criteria. Robustness in that case is understood as the insensitivity of the design’s performance against undesirable if not unexpected deviations from nominal parameters. These could arise from material property variations, inaccuracies in manufacturing and integration, possible settling effects due to launch loads, deviations from nominal status in final deployed state, or some non-nominal in-orbit loads. Effects of such small deviations must not amplify to unacceptable deviations in performance. This should be taken into account not only by the mechanical concept and material definition, but also by precision and quality in the manufacturing and integration processes.

In the following, meshes and CFRS surfaces are discussed, while membranes will be highlighted together with future large telescopes structures in a section further below.

3.2 Reflecting mesh surfaces

Mesh reflectors like those shown in Figs. 1, 3 or 5 of previous sections use pre-tensioned thin wire meshes as shown in Fig. 15. A prominent LDR example with considerable operational history is the AstroMesh reflector described by Thomson [58]. In fact, the AstroMesh architecture is a particular realization of the tension truss antenna concept invented by Miura, already presented in 1986 during the 37th IAF Congress and described in detail in [29], as well as similar constructions based on pantographs [25]. It consists of a pair of ring-stiffened, geodesic truss domes together with a deploying and stiffening ring truss deployed by a single cable. It achieves low total mass and also low stowed volume. A pair of doubly curved geodesic cable trusses, called *nets*, is placed back-to-back in tension across the rims of a deployable graphite-epoxy ring truss. The nets are made of unidirectional composite filaments called *webs*, attached in a pseudo-geodesic truss dome geometry. Webs can be configured to follow or approximate reflector contours as long as negative curvature is present. The ideal mathematical shape is approximated by flat, triangular facets that are formed when the mesh is stretched over the geodesic truss dome. Nevertheless, it is quoted that quite high surface accuracies can be achieved typically in the order of 1 mm RMS deviation for a 10-m diameter surface. Of course, the high number of facets then needed puts a considerable burden on manufacturing, integration, stowage and also reliable deployment of the then many cables needed for connecting the front to rear net. Possible thermal expansion depends on different effects. On facets level, thermal strain

superimposes in-plane to that of pre-tension. Resulting deviations in the reflecting surface then depend on the arrangement and thermal expansion of the other parts, including that of the nets connecting ties and also of the properties of the outer stiffening ring. The thermal strains in the reflecting surface also cause a change in internal residual forces originally generated by the pre-tensioning and also acting on nets and stiffening ring. This then gives rise to an overall shape deviation.

The thermo-elastic behavior of the AstroMesh general architecture has been addressed by Miura and Miyazaki in the detailed description of the tension truss antenna [29]. The sensitivities of thermal distortions resulting from cables elongations were analyzed. However, even if the net of cables is in principle statically determined, the tension state is not unique and, therefore, the tension is not necessarily controlled. This has led to evolutions of the network design, such as the ones proposed by You and Pellegrino [25] and Tibert and Pellegrino [26], in which both position and pretension are controlled. A rather simple isostatic network with control of position of nodes and tension in cables has been presented lately by Rodrigues [45] and is part of the recent developments [33, 44].

A typical mesh is made out of knitted molybdenum or tungsten wires with the core diameter of around 20 microns. Coating of each wire is made of gold layer over an intermediate layer of nickel. It gets its defined stiffness due to pre-tensioning. The complex mesh structure might generate a number of potential passive inter modulation (PIM) mechanisms due to possible relative sliding of wires, uncertainty of contact and also possible variations or degradations in wire coating. Relative sliding of wires could be generated, e.g., by micro-vibrations in orbit. Attenuation of such vibrations can be achieved by proper handling of the



Fig. 15 A typical metal wire mesh

excitation source and levels, by mistuning between resonance and excitation frequencies, or passive and active damping. While these measures are more or less related to the whole reflector assembly, proper pre-tension of the mesh of the reflector dish is required to achieve sufficient membrane stiffness also for considering such possible PIM effects. Typical values of such pre-tension are around 0.1–1 N/cm, also depending on the type of mesh and density of cable web it is attached to achieve the required facets.

Since metal materials of such meshes are less favorable for thermo-elastic stability, different efforts have been undertaken to minimize the coefficient of thermal expansion (CTE) and also PIM by investigating meshes composed, e.g., of aramid fibers and beryllium-copper [60]. Reduction of sensitivity of wave incident angles is achieved by special weaving techniques as described by Miura et al. [61]. The interaction of net and cable mesh is discussed by Di [62], where also optimization techniques are used for improving shape accuracy by proper adjustment of cables.

A further aspect related to the intrinsic nature of metal meshes, due to their pre-tension, is their inherent membrane anticlastic behavior. This results in the so-called pillowing effect between attachments, which is actually the dominating surface error of these antenna reflectors if not properly addressed. The cable networks, if present, allow to mitigate this effect to a certain extent, although not completely. It is, however, difficult to predict the magnitude and sensitivities of pillowing and it requires often non-linear analysis.

In the case of an umbrella-type reflector concept like that of IAI's Teccar radar reflector of Fig. 16, quite a number of radial stiffeners providing sufficient shape accuracy then might have to be used. Nevertheless, for the related RF wavelengths and available launch compartment space, this design concept was quite straightforward.

3.3 Carbon fiber reinforced silicone composites for precision reflecting surfaces

A new type of fiber composite reflecting material and surface has been created and developed at the Institute of Lightweight Structures (LLB) of Technische Universität München (TUM). The CFRS material is based on Carbon fibers supported by a soft silicone matrix. Some out of several possible LDR concepts made from CFRS are described by Datashvili in [63], while a detailed description of this material and its behavior is given in [64]. This material on the one hand has very good in-plane stiffness properties and low thermal expansion, and on the other hand it can be well folded and deployed quite easily for large surfaces. In contrast to meshes, these CFRS reflecting surfaces are not pre-tensioned, so no pillow effect occurs. This is achieved by assigning a small bending stiffness to



Fig. 16 Umbrella-type mesh reflector “Tecsar” from IAI [59]

the reflecting surface, allowing consideration of the reflecting surface material as a thin flexible “quasi” shell or shell-membrane. By this, higher surface accuracies can be obtained with even lower mass compared to the same structure with a mesh. A stress-free surface is achieved by joining the reflecting surface laying on its mold from top with the fully deployed backside and deploying structure, whatever type they are.

This reflecting CFRS shell-membrane fits to quite different types of reflector concepts, such as the one of Fig. 17. During “0 g” parabolic flights with an aircraft, photogrammetric surface geometry measurements carried out after many deployments demonstrated good shape accuracy and repeatability.

In a radially deploying concept such as that of Fig. 18, the deployment is achieved by radially deploying pantographs, which in their final deployment phase tension CFRS membrane ribs at the rear, but do not tension the reflecting surface per se. The tensioned rear membranes then provide overall stiffness and additional attachment points for the reflecting surface.

For the CFRS material, bi- and tri-axially woven fabrics are used in these cases. Figure 19 shows a closer view of a

tri-axially (0, +60, −60) woven type together with a micro- or meso-scale finite element model used for computational material design and characterization, complementary to experimental approaches. The space between silicon impregnated fiber bundles is kept empty, which saves mass and reduces acoustic launch loads and in-orbit solar pressure force.

Further relevant properties of this CFRS material are:

- Possibility of the use of a single layer due to its quasi-isotropy in case of tri-axial weave.
- Very low aerial density of a single layer due to its lattice (porous) structure and, therefore, ultra lightweight designs are possible.
- Porosity helps in decreasing the response on acoustic loads and through thickness thermal gradients in a structure.

Attractive properties of the silicone matrix material are:

- low glass transition temperature T_g around -110 °C,
- highly flexible above this temperature,
- very low outgassing and volatile contents,
- no moisture uptake,
- resistivity to ultraviolet radiation, electron radiation and atomic oxygen,
- wide range of service temperatures possible (-200 to over 250 °C),
- possibility of curing at room temperature,
- extremely low shrinkage during curing.

In Fig. 20, a typical expansion behavior together with related CTE data at different temperature ranges is given. Between -105 °C up to $+150$ °C the effective CTE is around -0.36×10^{-6} because of the dominating fiber effects. Below around -105 °C, it increases to 3.8×10^{-6} caused by the silicone’s stiffening and thus higher influence below its glass transition temperature T_g . The different signs in CTE as function of temperature result into a very small effective CTE value of around 0.7×10^{-7} in a temperature range from RT down to -170 °C.

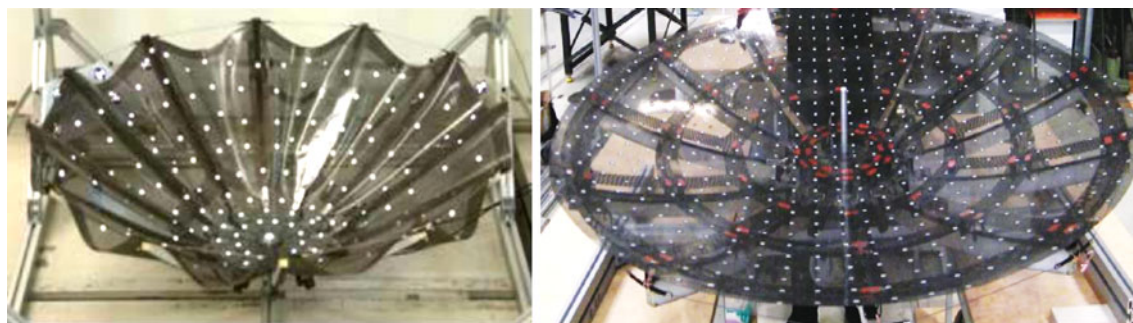


Fig. 17 An umbrella-type reflector with CFRS reflecting surface and CFRP radially stiffening sandwich ribs and with white markers for photogrammetric measurements [63]

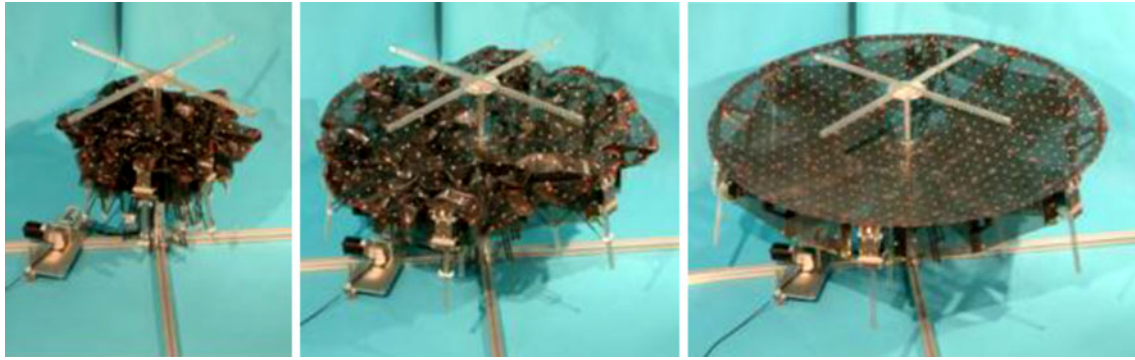


Fig. 18 An umbrella-type reflector with CFRS reflecting surface and CFRP radially stiffening sandwich ribs together with white markers for photogrammetric measurements [63]. Courtesy of TUM and ESA

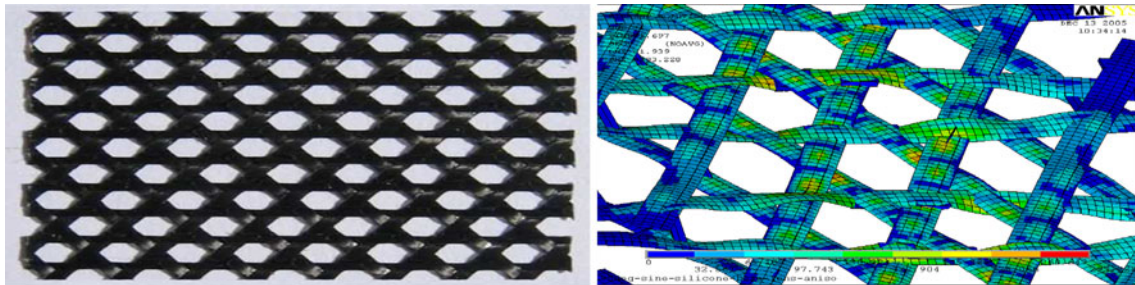


Fig. 19 Tri-axially woven Carbon fabric imbedded in silicone around the fiber bundles (*left*) together with meso-scale finite element model (*right*) [64]

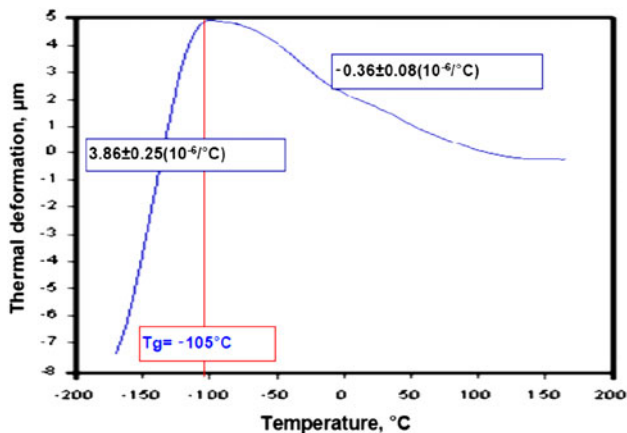


Fig. 20 Thermal expansion properties of CFRS vs. temperature [64]

Folding and deployment tests with specimen show that this can be done many times at temperatures above $-100\text{ }^{\circ}\text{C}$, with no indication of creases or creep if too small bending radii for brittle fibers are avoided. Even after several hundred thermal cycles between $-160\text{ }^{\circ}\text{C}$ and $+110\text{ }^{\circ}\text{C}$, no degradation of thermal and mechanical properties and no micro-cracks could be observed.

Some measured RF properties are given in Table 1, showing that related properties are roughly comparable to those of CFRP.

For further enhancement of surface reflectivity properties, preliminary trials for coating CFRS surfaces with a thin Aluminum layer provide quite satisfactory results [72]. PIM could be reduced below specified thresholds by inclusion of silver particles in the silicone matrix.

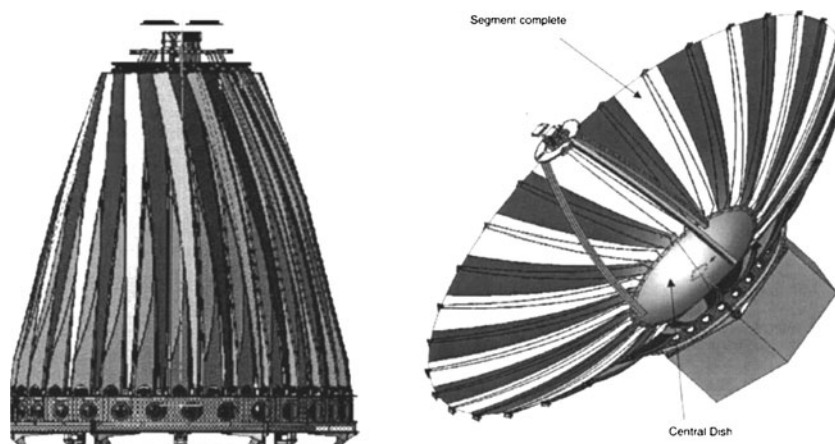
In current research and technology studies, such a CFRS reflecting surface with a diameter close to 6 m will be manufactured and thermo-mechanically tested in ESTEC's LSS chamber together with its circumferential truss structure providing overall stiffness.

3.4 Deployable stiff panels

In the context of reflecting surfaces, deploying *rigid* panels like those shown in Fig. 21 shall be also mentioned. The deployment scheme is basically quite similar to that of a Daisy flower. The CFRP panels are made out of high stiffness and low CTE Carbon fibers, thus providing good thermo-elastic stability and good manufacturing accuracy. Drawbacks are the relatively high stowage volume and possibly also higher aerial mass density, since also deployment mechanisms and provisions of proper end positions of the panels after deployment have to be taken into account as well. Nevertheless, they are an option to be considered when it comes to space telescope reflectors.

Table 1 Measured RF properties for CFRS reflecting surface

Subject/RF-requirement	TWF to CFRS
Reflection loss <0.1 dB	0.05 to 0.13
Depolarization <-40 dB	<-47 to -42
Amplitude variation for 2 orth. polarizations <0.02 dB	<0.02
Phase variation for 2 orthogonal polarizations <2°	<0.5°
Transmission coefficient <-20 dB	-33 to -21

Fig. 21 A concept with deployable stiff panels [65]

3.5 Large deployable space telescope reflectors and membrane reflecting surfaces

For large telescope reflectors and mirrors, shape accuracy determined by manufacturing, deployment and ultra-low in-orbit expansion is an even more stringent requirement. So apart from deploying stiff panels, membranes and shell-membranes possibly together with extensive shape control are intensively investigated. Before addressing this in some detail, first a brief view in current state of the art is given.

Current high precision space reflectors and mirrors have a diameter either still fitting into larger launcher payload bays or have some “mild” deployment technique like that of the James Webb telescope. The materials usually are stiff, lightweight, thermo-elastically stable with good thermal conductivity. In addition, surface roughness shall be low, and good reflectivity is to be achieved by proper coating.

For stiff reflectors, ultra-low expansion (ULE) glass from the past has been partly substituted for certain wavelengths by the lighter silicon carbide (SiC). This material combines high thermal stability and high specific stiffness with good optical properties [66]. Moreover, it is a quite homogenous material, in contrast to CFRP where fiber print-through would have to be avoided. The Herschel spacecraft, launched in 2009, is for the time being the largest space IR telescope with a primary SiC mirror of 3.5-m diameter and still an areal density of 22 kg/m² [67]. This is far away from being reasonably up-scalable geometrically to a 10-m diameter range and above, even if appropriate stowage and deployment

concepts would be available. However, it is believed that the potential exists to build 2–3 m segments of SiC with areal densities down to several kg/m² only. Silicon carbide reinforced with (randomly distributed) Carbon fibers (C/SiC) has less brittleness than pure SiC and generates much smaller volume shrinkage during processing [51].

For the James Webb Space telescope with a diameter of around 6 m, partly deployable Beryllium petals with an aerial mass density around 15 kg/m² are used [76] together with some means of in-orbit shape control, as briefly discussed later.

It is obvious that geometrical up-scaling of currently used mirror technology to obtain large mirrors would pose tremendous mass problems, apart from defining proper concepts for stowage and precision deployment. In a longer term, candidates for low aerial density reflectors are Gosamer structures which consist of membranes or thin shells. The application of current concepts in telescopes would require the creation of three dimensionally curved surfaces that focalize light by reflection. These require shape accuracies in the order of a tenth of a wavelength despite thermal and other disturbances. The MEVICON concept consists of Kapton films 125 μm thick which are stiffened by the double-curved shape [68]. The achieved shape accuracy also based on shape control techniques of 1-m diameter prototypes is impressive, but sufficient shape accuracy for large reflectors still has to be proven. Further interesting investigations of thin films with low CTE are reported, e.g., in [69] with emphasis also on required high precision tooling, e.g., of molds and related cost issues. In

most cases, deployment has to be followed by space rigidization and also intensive shape control efforts [70].

Special concepts on large diffracting apertures have been proposed for space telescopes and Earth observation [71]. A system with 25-m diameter for Earth observation at geostationary orbit can be envisaged based on a Fresnel lens constituted of some kind of plastic film. Instead of circular grooves like in classical Fresnel principle, many ten thousands or more of holes per square meter are to be drilled into the then “photon sieving” surface. Stretching of the film and maintaining an optical figure of 1 mm can be envisaged by boundary actuation or by distributed piezoelectric actuation. But as discussed in [72], several technological obstacles are still to overcome such as proper drilling processes for the holes which also avoid residual thermal stresses possibly causing warping around hole boundaries. Also provision of proper surface tensioning in orbit is nontrivial because of the high density of holes in a flexible material. LDRs based on deployable rings and highly accurate CFRS surfaces together with reflecting coating and shape control might be applicable for photon collimators [72].

4 Shape adjustment and shape control

In-orbit shape control requires proper sensing and actuating techniques together with a control loop. Since complexity then significantly increases, the so-called post-manufacturing adjustment as a first step is also briefly discussed. In that case, shape deviations caused, e.g., by residual stresses generated during manufacturing are to be compensated to the best possible extent by adding special compensation devices which are to be triggered more or less only once at ground.

The general idea behind both on-ground shape adjustment and in-orbit shape control can be also derived from the shape error minimization problem

Minimize

$$f = \sum_i \left(d_i - \sum_j u_{ij} x_j \right)^2, \quad i = 1, \dots, m, \quad j = 1, \dots, n,$$

where d_i is the shape error at a reference point i of total m reference points, and u_{ij} is the deformation at this reference point i due to a unit stroke at actuator position j with a total of n actuators. The solutions x_j then are the actual actuator strokes to be applied. In case of a linear structure, or more strictly speaking a linear relation between actuator strokes and induced corrective deformations, the solution results from solving a linear least squares problem. In nonlinear cases, the actuator influence matrix u_{ij} might have to be established at proper reference deformations and possibly be updated stepwise. Essentials for implementation are the selection of proper low mass and low volume

actuators and their positioning to provide the required set of strokes $\{x\}$ to be smoothly introduced into the reflecting surface. Moreover, spurious effects of control actuators like local temperature increase or higher CTE have to be minimized.

4.1 On-ground post-manufacturing shape adjustment

To reduce manufacturing shape errors, compensation devices based on different means such as shimming or certain tension–compression devices can be used. These devices provide the (fixed) strokes x_i for properly enforced displacements u_{ij} in the basic equation given above.

A possible type of such devices could be shape memory materials attached to the structure at proper positions. Apart from shape memory alloys (SMA) also shape memory polymers (SMPs) have been investigated for that purpose [73]. Such SMPs show a one-way-shape memory effect, which can be described by a thermo-mechanical cycle. SMPs can be manufactured with conventional curing cycles in nearly arbitrary shape. By heating the material above its transition temperature T_{Trans} , its Young’s modulus E drops down and it can be easily mechanically deformed. Cooling down the material in this mechanically constrained state, the deformation freezes in. This process is called *programming* and ends up with the programmed, temporary shape. By heating up the material above the transition temperature again, the shape recovery starts and the material returns to its original, permanent shape. When an SMP patch is fixed to a part or structure and triggered, its free expansion is constrained which causes the required actuation forces. The physical–chemical background of SMPs together with procedures and results for their thermo-mechanical characterization is described by Leng and Du [74] and Bar-Cohen [75]. In short, advantages of SMPs are their low mass and good compatibility with typical reflector base materials. On the other side, possible creep of the SMP and with that a reduction of actuation forces over time might be a problem especially at higher operational temperatures and temperature variations. These are possibly overcome by the inclusion of fillers and nano-particles, or alternatively by the use of other types of shape memory materials or small adjustment actuators.

For experimental verification of such adjustment approach, four different types of SMP actuators with different geometry and different positions are attached onto a CFRP plate structure supposed to be planar but in fact is significantly curved by intention due to curing stresses. By actuating these SMPs by moderate temperatures, this deviated curved shape is to be brought back to planarity as close as possible. Typical results of this shape adjustment technique are shown in Fig. 22.

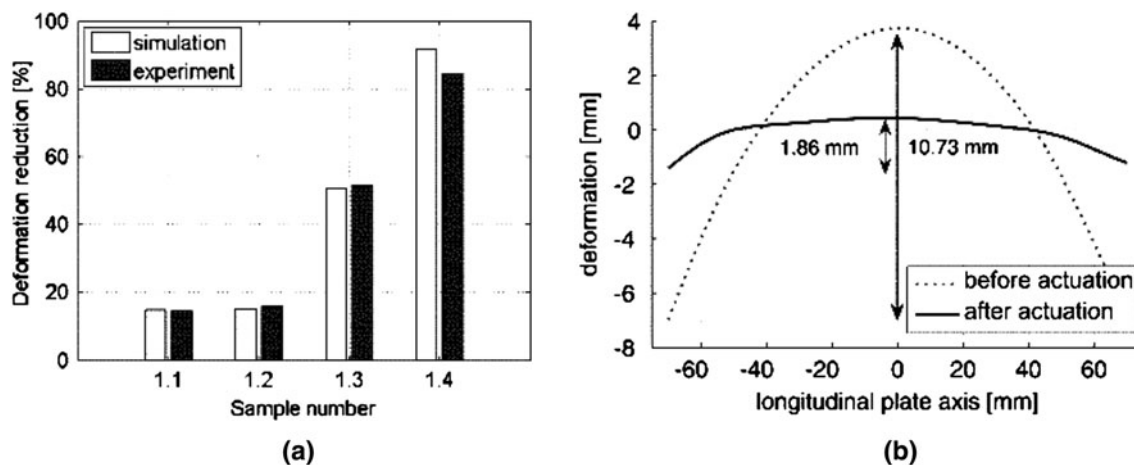


Fig. 22 **a** Summary of CFRP plate shape error reduction results; **b** shape contour of a plate sample before and after shape memory polymer patch actuation [73]

As can be seen from Fig. 22, a considerable improvement in shape accuracy could be achieved, also with good correlation of experimental with simulation results. For the latter, finite element modeling is used for this adjustment process with SMP actuation models based on the analogy between thermal and shape memory expansion.

4.2 In-orbit shape control

Shape control of highly precise space reflectors has to keep shape deviations caused by quasi-static or low frequency disturbances such as different temperature loads to a minimum. Since requirements on shape precision often are in the range of μm or even lower, flexible reflecting surfaces then also require only small actuating forces generated by lightweight micro-actuators. The actuator forces have to be introduced smoothly in order to avoid local negative effects on shape accuracy. In addition, the shape control system and especially its actuators have to work under severe environmental conditions. This might be one reason why active shape control for space reflectors is far less matured than that for reflectors or mirrors of large ground telescopes.

A first practical application of shape control of highly precise space reflectors or telescope mirrors will be the main mirror of the James Webb Space Telescope, see for example [76]. This reflector is composed of many hexagon panels made out of beryllium alloy. Since the mirror diameter exceeds that of the launcher's fairing, the outer panels are to be deployed in space into their final position. During operation, rigid body and elastic displacements of the panels are controlled even under cryogenic temperature by actuators placed on their backside. Smooth actuator load introduction is achieved by properly distributed actuators on each panel, together with what is called "load spreaders" interfacing the actuators and mirror panel structures.

4.2.1 Shape-controlled membrane reflectors and use of PVDF actuators

A number of smart materials have been proposed in the literature as candidates for sensor and even more so for actuator elements. Examples include piezoelectric ceramics and a variety of piezo-electric polymers such as polyvinylidene fluoride (PVDF), SMA, and also fiber optics for sensing. In all cases, couplings between the mechanical, electrical, magnetic, or thermal properties of the materials to the applied stimuli must be adequately modeled. To date, understanding of the coupling between these properties has been based more on experimental evidence and less on analytical models. This is because, in most cases, the nature of the coupling is rather complex and maybe nonlinear. Selective actuation of distributed PVDF sectors of a circular membrane was found to be effective [77, 78]. The use of PVDF actuation for CFRS reflecting surfaces as described in previous sections has been also investigated with initial results reported in [72]. The in-plane stiffness of CFRS makes PVDF less effective, and the higher CTE and temperature sensitivity of PVDF also have to be taken into account as a possible undesirable effect.

Along with progress in such smart structures and material technology, adaptive/active control laws have also evolved. There is extensive literature on the subject such as in [78–80], in which a variety of control strategies and optimal sensor/actuator placement methodologies are explored. Consideration of nonlinear structural behavior and adaptive control parameters to be updated via a learning process during use are some of the features discussed. The performance of truly large membrane apertures is largely influenced by the details of the local as well as global features of the membrane, and aberrations thereof. In this regard, it is essential that the predictive models are

able to capture such local details together with long-term behavior. In the end, proper actuators and actuation devices are a key point for operating reliably over a longer time period under severe space conditions. Their control authority or actuation efficiency shall be sufficiently high, which is not easy to achieve for actuators directly attached to a (membrane) surface. Spurious actuator effects generated, e.g., by local “hot” spots or higher thermal expansion shall be minimized.

According to the required sensing and control input signals, the Shack–Hartmann sensor is an elegant means for measuring the shape of a wave front. This technique has found application to a wide variety of applications. A complementary concept are fiber optic strain sensors (FOS) integrated into or attached onto the rear of the reflector which measure strains at many locations. These strains then are taken to reconstruct displacement fields to be used as input to shape control loops. This reconstruction is carried out via proper transfer matrices [C], which couples the set of measured strains with a large and dense set of discrete and thus quasi-continuous displacements [81]. The transfer matrix [C] can be established via simulation, experiments, or combinations thereof. Proper integration of the optical fiber based Bragg sensors into the usually very thin reflective layers is a challenging task as well, where influence of the mounting or bonding devices has to be kept sufficiently small.

4.2.2 Consideration of in-orbit dynamics and micro-vibration attenuation

Possible elasto-dynamic interaction of the reflector assembly with the satellite bus might have to be considered as well for the often highly flexible reflector assemblies. In general, lower bounds for fundamental frequencies have to be observed. The assembly of reflector and deployment arm needs attention due to the mass and mass moment of inertia of the reflector attached at the end of the deployment “beam”. Apart from the provision of sufficient stiffness, introduction of passive and active damping might be a further option. While passive vibration attenuation and damping look straightforward and in contrast to active means also do not need external sources or sensors, local temperature and CTE hotspots or stick–slip are to be avoided. The basics of active damping are well described for example in [82] and [83]. Such active damping is especially relevant again for the reflector interface to the satellite bus, being either a mounting structure or a quite lengthy boom. The actuators for active damping should be positioned at areas of relatively high modal energy. For strain inducing actuators, this usually means areas of relatively high (modal) strain energy, while for more or less laterally acting actuators these are areas of relatively high

kinetic energy. This actuator positioning task can be handled more strictly by certain controllability measures, see also Preumont [83]. Such procedures should be complemented by engineering insight, and vice versa.

4.2.3 Parameterized model order reduction for in-orbit vibration control simulation

For simulating in-orbit structure-control interaction, dynamic simulation models often are to be used with significant order reduction. An overview on such reduction methods can be, e.g., found in [84]. But it is rarely observed that due to the usual modifications of parameters of such structures during their development process, model reductions would have to be repeatedly carried out again. Since model reduction per se is computationally quite costly as well, methods providing *parameterized* reduced models with explicit access to design parameters in the reduced model space are in order then, see for example Antoulas and Sorensen [85]. Further improvements of such techniques are given by Yoo and Baier [86] and Yoo [87] with applications in shape control and active damping simulations of space reflectors and solar arrays, respectively. Model reductions down to even less than 1 % of the original model size have been carried out with parameterizations on material and geometrical structural properties. Simulation results obtained from such parameterized reduced order models then are still quite close to those of the original models even for parameter changes up to around 50 %.

5 Shape reconfiguring reflectors

Communication satellites might require reconfiguration of their radiation pattern to adapt to modified mission needs. This can be achieved, e.g., by proper control of multiply fed RF beams, or alternatively by drastic yet precise reflector shape reconfiguration or shape morphing. If technically feasible, the latter might be more flexible and less costly. Because such shape modifications may require relatively high spatial frequencies and amplitudes possibly up to the cm-range with high precision, challenging requirements exist for such reconfigurable surfaces together with their actuation mechanisms.

5.1 Mechanical requirements

Since these functional requirements include out-of-plane reshaping amplitudes often at least one order larger than the thickness of the reflecting surface thickness, possible geometric nonlinearity might have to be taken into account. Again a good passive intermodulation (PIM)

behavior and good reflectivity of surface materials are needed as well as a sufficiently high accuracy of the reshaped surface.

Essential mechanical properties needed for the reconfigurable surfaces are:

- low to moderate tensile modulus,
- low, even close to zero, shear modulus,
- moderate bending stiffness in combination to the previous two properties and with a certain high ratio to the shear modulus.

Low shear modulus is a key, since it results into the required flexibility with low actuator forces, while moderate bending stiffness results into morphed shapes with smooth curvature change. As will be addressed below, very thin wire nets and also CFRS reflecting surfaces are options to be considered.

5.2 Concepts of shape reconfiguring reflectors

Different investigations were performed to create such mechanically reconfigurable reflector. In a pioneering work of Clarricoats, the reshaping of a rim supported metal tricot mesh surface was investigated [88]. A further concept is the orthogonal interwoven steel wire grid [89] which shows a good mechanical performance. Its reshaping is accommodated through the out-of-plane bending and in-plane translations and rotations among its members. It can be reshaped in relatively large amplitudes compared to its thickness. Unfortunately still low PIM performance blocks the successful usage of such concepts, unless further treatments such as special coating are foreseen.

Another novel development direction is the use of flexible fiber composite materials such as CFRS discussed in previous sections. As shown in [90, 91], CFRS materials can well satisfy the mechanical requirements mentioned. It is then important to avoid statically over-determinate fixation, then. For further improved RF properties, certain

doping of the silicone matrix with silver particles is carried out [92].

5.3 Laboratory model testing and analysis-test correlation

For further verification of a CFRS concept, a demonstration model of about 0.8-m diameter has been developed (Fig. 23). For this, the positioning of the actuators is set to be quite regular since there is no real position preference to be expected for the very different sets of goal shapes. This is also in line with results obtained by Washington [93]. A set of goal shapes to be achieved by geometric reconfiguration have been determined in advance by RF analyses. The needed actuator displacement strokes are obtained from solving a least squares error problem minimizing the difference between shapes generated by these strokes and the defined goal shapes. Certain other constraints like technical limits of the actuator stroke amplitudes are considered as well [91].

The reflective surface is made out of two continuous CFRS layers and additional CFRS patches on the rear side around the actuator connection points to provide smooth actuator load introduction. Because this skin design requires actuator forces not exceeding the range of some Newton, micro-actuators can be applied with mass of typically much less than 50 g each. This is important because required actuators density might easily reach around 50 per square meter, also depending on the complexity of the goal shapes to be achieved.

The deformed shapes were measured by photogrammetry and compared to the simulated shape. From Fig. 24, the good matching between these gets obvious. The overall RMS shape difference between simulation and test is less than 0.2 mm. The tests also revealed several relevant details, e.g., with respect to the required precise alignment of actuators. Also special measurement techniques have been applied to cover the behavior over the full range of

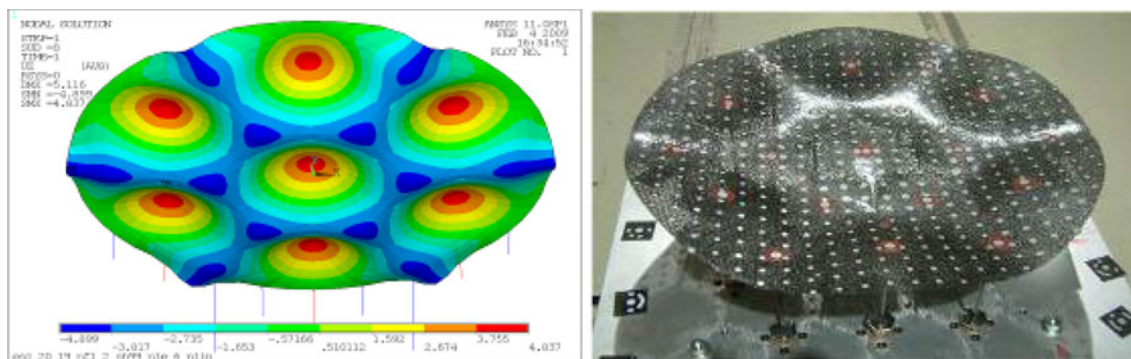


Fig. 23 Simulation (*left*) and demonstration model (*right*) being morphed from initial parabolic shape to a specified goal shape. Courtesy of TUM and ESA [90]

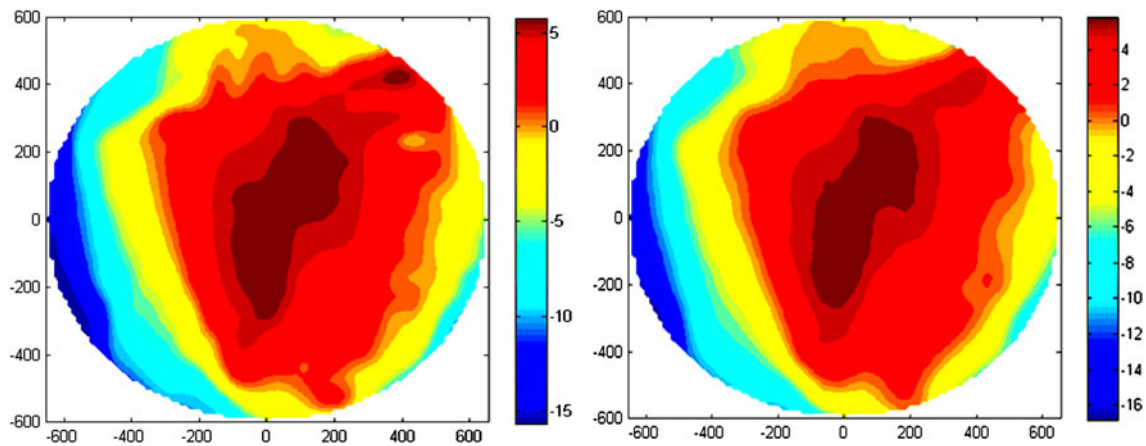


Fig. 24 Isocontours of a morphed actual shape (*left*) and a goal shape (*right*) [91]

shape morphing, which relates to deformations, strains and also actuator force levels [90].

Further improvements could be achieved by applying coupled electric-mechanical simulations for actuator stroke determination [93, 94]. This resulted into even better RF performance and/or also into a smaller number of actuators and/or even smaller induced stresses in the reconfigured reflecting surface.

6 Summary and conclusions

A review of general concepts, the state of the art and recent advances in large deployable apertures for space applications have been presented. The main applications addressed include satellite telecommunications for Fixed and Broadcasting Satellite Services and Broadband Satellite Services, as well as air traffic management satellite services, emergency and tactical communications systems. This results in required apertures from 5 to 25 m operating in frequencies from VHF to Ka band. Earth observation missions can also be enabled, mainly reflector-based SAR and radiometry, as well as radio-astronomy and other scientific applications.

Deployable structures have been classified from the point of view of their kinematics. The deployment of structural mechanisms is classified as planar and three-dimensional and the different types and variants are discussed in view of their characteristics with respect to deployable apertures. Open and closed chains are discussed, with special emphasis to mobility and degrees of freedom and the importance of their control and robustness. The particular family of overconstrained nR bar linkage mechanisms has been used as benchmark for the study of degrees of freedom in more depth and the extrapolation of these ideas to other

mechanisms, to control the deployment process and the stability in a space environment. New developments addressing the concepts of increased mobility have been presented, in particular the conical rings based on V-folding bars and pantographs. Actuation and synchronization have been addressed in relation to the degrees of freedom. It has been concluded that the knowledge of these aspects can be fundamental for the verification of reliability and stability of the deployable structures.

Highly flexible structures have been discussed in the context of large deployable surfaces with low aerial density and high thermo-elastic stability. Several types of surfaces are described, including the classical metal knitted meshes and the recently developed shell-membranes based on CFRP and CFRS. The intended applications addressed include the future developments of large telescopes with higher structural efficiency and the reconfigurable optics of telecommunications antennas. An introduction to the shape adjustment and control of surfaces by implementation of shape memory materials and piezo-electric polymers has been provided, paying attention to the matching to the surface structural configurations and thermo-elastic stability.

These particular disciplines are still in rapid development and further consolidation will happen in the near future, enabling the mentioned applications with higher reliability and increased performances. Such progress will be also complemented by further improvements in modeling and testing of such large structures.

Acknowledgments The authors would like to acknowledge the continued support from the ESA technical and applications directorates, in particular the mechanical and electrical departments of ESTEC. Special thanks to Dr. W. Kordulla and Dr. C. Stavrinidis for making possible this special edition of the CEAS Space Journal.

References

- Mangenot, C., et al.: Large Antenna Working Group, ESA Final Report, TEC-EEA/2010.595/CM (2010)
- Amyotte, E., Martins Camelo, L.: Antennas for satellite communications. In: Imbriale, W., Gao, S., Boccia, L. (eds.) *Space Antenna Handbook*, Chap. 12. Wiley, New York (2012)
- Capece, P., Torre, A.: SAR antennas. In: Imbriale, W., Gao, S., Boccia, L. (eds.) *Space Antenna Handbook*, Chap. 13. Wiley, New York (2012)
- BIOMASS—Report for Mission Selection: An Earth Explorer to Observe Forest Biomass, ESA SP-1324/1 (2013). <http://www.esa.int/livingplanet>
- Meschini, A., Milano, M., Rigato, R., Cammarata, A., Santiago-Prowald, J.: Orbital manoeuvre disturbances of a large deployable antenna. In: *International Scientific Conference on Advanced Lightweight Structures and Reflector Antennas*, 14–16 October 2009, Tbilisi, Georgia
- Puig, L., Barton, A., Rando, N.: A review on large deployable structures for astrophysics missions. *Acta Astronaut.* **67**, 12–26 (2010)
- Medzmariashvili, E.: *Transformable Space and Ground Constructions*. Valemar S&T Ltd—Gregory & Co., Georgia (1995). (in Russian)
- Medzmariashvili, E., Kinteraya, G., Datashvili, L., Bedukadze, G., Siradze, N., Efremov, I., Chernyavski, A., Kravchenko, Y.: Space experiment “Reflector” on testing the large-scale deployable high precision offset antenna reflector of a new generation at the orbital station MIR. In: *AP2000 Millennium Conference on Antennas & Propagation*, Davos, Switzerland, 9–14 April 2000
- Scialino, G.L., Cherniavski, A., Korneev, V., Magjanov, R., Medzmariashvili, E., Gulyayev, V., Scolamiero, L., Santiago-Prowald, J.: Presentation of Reflector Dish Development Activities and Achieved Performances, 28th ESA Antenna Workshop, June 2005, ESA-ESTEC, Noordwijk, The Netherlands
- Roederer, A.: Historical overview of the development of space antennas. In: Imbriale, W., Gao, S., Boccia, L. (eds.) *Space Antenna Handbook*, chap. 7. Wiley, New York (2012)
- Pellegrino, S. (ed.): *Deployable structures in engineering, in deployable structures*. CISM Courses and Lectures, vol. 412. International Center for Mechanical Sciences. Springer, Berlin (2001)
- Datashvili, L.: Review and evaluation of the existing designs/technologies for space large deployable apertures. In: *International Scientific Conference on Advanced Lightweight Structures and Reflector Antennas*, 14–16 October 2009, Tbilisi, Georgia
- Ozawa, S., Shintate, K., Tsujihata, A.: Tri-fold deployable reflector for communication satellites. In: *AIAA 29th International Communications Satellite Systems Conference (ICSSC-2011)*. AIAA2011-8082
- Arkhipov, M., Fedorchuk, S., Kardashev, N., Vinogradov, I.: “RadioAstron”: the largest space deployable solid reflector antenna. In: *33rd ESA Antenna Workshop*, October 2011 ESA-ESTEC, Noordwijk, The Netherlands
- Sarrus, P.F.: Note sur la transformation des mouvements rectilignes alternatifs, en mouvements circulaires; et reciproquement. *Acad. Sci.* **36**, 1036–1038 (1853)
- Bennett, G.T.: A new mechanism. *Engineering* **76**, 777–778 (1903)
- Chen, Y., You, Z.: Spatial overconstrained linkages—the lost jade. In: Koetsier, T., Ceccarelli, M. (eds.) *Explorations in the History of Machines and Mechanisms*. Proceedings of HMM2012 History of Mechanism and Machine Science, vol. 15, pp. 535–550. Springer, Berlin (2012)
- Baker, E.J.: The Bennett, Goldberg and Myard linkages-in perspective. *J. Mech. Mach. Theory.* **14**, 239–253 (1979)
- Chen, Y.: *Design of Structural Mechanisms*. PhD thesis dissertation, University of Oxford (2003)
- Goldberg, M.: New five-bar and six-bar linkages in three dimensions. *Trans. ASME* **65**, 649–663 (1943)
- Myard, F.E.: Contribution à la géométrie des systèmes articulés. *Société Mathématique de France* **59**, 183–210 (1931)
- Fraux, V., Lawton, M., Reveles, J.R., You, Z.: Novel large deployable antenna backing structure concepts for foldable reflectors. In: *Large Deployable Antenna Workshop*, 2–3 October 2012, ESA-ESTEC, Noordwijk, The Netherlands
- Qi, X., Li, B., Deng, Z., Liu, R., Guo, H.: Design and optimisation of large deployable mechanism constructed by Myard linkages. In: *Large Deployable Antenna Workshop*, 2–3 October 2012, ESA-ESTEC, Noordwijk, The Netherlands
- Fanning, P., Hollaway, L.: The modal analysis of a unit building block for a 5 metre deployable antenna for space applications. In: *Proceedings of the 4th International Conference on Space structures*, vol. 1, pp. 432–441. *Space Structures 4*, Surrey (1993)
- You, Z.: *Deployable Structures for Masts and Reflector Antennas*. PhD thesis dissertation, University of Cambridge (1994)
- Tibert, G.: *Deployable Tensegrity Structures for Space Applications*. Doctoral thesis, KTH Royal Institute of Technology Department of Mechanics, Stockholm (2002)
- Ganga, P.L., Zolesi, V., Scolamiero, L., Micheletti, A., Podio-Guidugli, P., Tibert, G., Donati, A., Ghiozzi, M.: Tensegrity structures for large deployable reflectors. In: *Large Deployable Antenna Workshop*, 2–3 October 2012, ESA-ESTEC, Noordwijk, The Netherlands
- Narayanan, S.: *Space Structures: Principles and Practice*, vol. 2. Multi-Science Publishing Co. Ltd., Essex. ISBN: 0 906522 42 0 (2006)
- Miura, K., Miyazaki, Y.: Concept of the tension truss antenna. *AIAA J.* **28**(6), 1098–1104 (1990)
- Hirosawa, H., et al.: Space VLBI satellite HALCA and its engineering accomplishments. *Acta Astronaut.* **50**(5), 301–309 (2002)
- Thomson, M., Marks, G., Hedgepeth, J.: *Light-Weight Reflector for Concentrating Radiation*. Patent US5680145 (1997)
- Thomson, M.: The AstroMesh deployable reflector. In: Pellegrino, S., Guest, S.D. (eds.) *IUTAM-IASS Symposium on Deployable Structures: Theory and Applications* (Cambridge, UK, 6–9 September 1998), pp. 435–446. Kluwer Academic Publishers, Dordrecht (2000)
- Medzmariashvili, E.: Constructive logic of reflector created with double pantograph deployable load-bearing ring. In: *Large Deployable Antenna Workshop*, 2–3 October 2012, ESA-ESTEC, Noordwijk, The Netherlands
- You, Z., Pellegrino, S.: Structural concept of a deployable mesh reflector. In: *ESA Antenna Workshop*, ESA-WPP-100 (1995)
- Harris Corporation: *Development of the 15 metre Diameter Hoop Column Antenna*, NASA-CR-4038 (1986)
- Mini, F., Scialino, G.L., Milano, M., Lubrano, V., Conforto, P., Pellegrino, P., Caswell, D., Santiago Prowald, J., Van’t Klooster, C.G.M., Cherniavski, A., Korneev, V., Vorobey, I., Fedoseev, A.: European large deployable antenna: development status and applications. In: *Proceedings of the European Conference on Antennas and Propagation ‘EuCAP 2006’*, Nice, France, 6–10 November 2006 (ESA Publication SP-626, October 2006)
- Santiago-Prowald, J.: *Large Deployable Antennas Mechanical Concepts*. <http://www.kiss.caltech.edu/workshops/apertures2008/talks/santiagoprowald.pdf>
- Datashvili, L.: Foldability aspects of hinged-rod systems applicable to the deployable space structures. In: *Large Deployable Antenna Workshop*, 2–3 October 2012, ESA-ESTEC, Noordwijk, The Netherlands
- Datashvili, L., Endler, S., Baier, H., Langer, H., Friemel, M., Tsignadze, N., Santiago-Prowald, J.: Study of mechanical architectures of large deployable space antenna apertures: from design

- to tests. In: Large Deployable Antenna Workshop, 2–3 October 2012, ESA-ESTEC, Noordwijk, The Netherlands
40. Meguro, A., Mitsugi, J., Ando, K.: Modular Deployable Antenna. Patent US62023791 (2001)
 41. Meguro, A., Shintate, K., Usui, M., Tsujihata, A.: In-orbit deployment characteristics of large deployable antenna reflector onboard engineering test satellite VIII. *Acta Astronaut.* **65**, 1306–1316 (2009)
 42. Kellog, K.: Presentation on Galileo Antenna Failure and Mission Recovery. Jet Propulsion Laboratory/CalTech, USA (1995)
 43. Santiago-Prowald, J., Such Taboada, M.: Innovative deployable reflector design. In: 33rd ESA Antenna Workshop, October 2011 ESA-ESTEC, Noordwijk, The Netherlands
 44. Medzmariashvili, N., Medzmariashvili, E., Tsignadze, N., Tusishvili, O., Santiago-Prowald, J., Manganot, C., Baier, H., Scialino, L., Philipenko, L.: Possible options for jointly deploying a ring provided with v-fold bars and a flexible pre-stressed center. In: Large Deployable Antenna Workshop, 2–3 October 2012, ESA-ESTEC, Noordwijk, The Netherlands
 45. Rodrigues, G., Such-Taboada, M., Datashvili, L., Tsignadze, N., Medzmariashvili, E., Santiago-Prowald, J.: Isostatic cable net for large deployable antenna reflector. In: Large Deployable Antenna Workshop, 2–3 October 2012, ESA-ESTEC, Noordwijk, The Netherlands
 46. Tserodze, S., Medzmariashvili, E., Tusishvili, O., Tsignadze, N., Santiago-Prowald, J., Van 't Klooster, C.: Mechanical supporting ring structure. In: Large Deployable Antenna Workshop, 2–3 October 2012, ESA-ESTEC, Noordwijk, The Netherlands
 47. Scialino, L., Migliorelli, M., Gatti, N., Breunig, E., Ihle, A., Datashvili, L., van 't Klooster, K., Santiago Prowald, J.: Reflector technology trade-off for lda on telecom and earth observation applications. In: Large Deployable Antenna Workshop, 2–3 October 2012, ESA-ESTEC, Noordwijk, The Netherlands
 48. Ihle, A., Breunig, E., Datashvili, L., Migliorelli, M., Scialino, L., van't Klooster, K., Santiago-Prowald, J.: Large deployable reflector technologies for future european telecom and earth observation missions. In: Large Deployable Antenna Workshop, 2–3 October 2012, ESA-ESTEC, Noordwijk, The Netherlands
 49. Frank Pai, P.: Highly Flexible Structures: Modelling, Computation and Experimentation. AIAA Education Series (2007)
 50. Santiago-Prowald, J., Henriksen, T., Stavrinidis, C.: Modelling and testing of large deployable space apertures. In: Proceedings of the International Scientific Conference “Advanced Lightweight Structures and Reflector Antennas”, 14–16 October 2009, Tbilisi, Georgia
 51. Santiago-Prowald, J., Salghetti Drioli, L.: Space environment and materials. In: Imbriale, W., Gao, S., Boccia, L. (eds.) *Space Antenna Handbook*, Chap. 4. Wiley, New York (2012)
 52. Tan, L.T., Soykasap, O., Pellegrino, S.: Design and manufacture of stiffened spring back reflector demonstrator. In: Proceedings of the 46th AIAA/ASME/ASCE/AHS/ASC Structures, Structural Dynamics and Materials Conference, April 2005, AIAA 2005-2048
 53. Baier, H., Darashvili, L., Nathrath, N., Pellegrino, S.: Technical Assessment of High Accuracy Large Space Borne Reflector Antenna. Final Report, Contract16757/02/NL/LvH/bj
 54. Baier, H., Darashvili, L., Nathrath, N.: The deployable precision flexible shell-membrane reflector SMART. In: Proceedings EuCAP 2006, Nice, France, ESA SP-626 (2006)
 55. Mallikarachchi, H.M.Y.C., Pellegrino, S.: Composite deployable tubular antenna booms. In: Large Deployable Antenna Workshop, 2–3 October 2012, ESA-ESTEC, Noordwijk, The Netherlands
 56. Schmidt, T., Schiller, M., Schmalbach, M., Fix, A., Scolamiero, L.: Recent EM testing results for ultra-light deployment mechanism for sectioned large deployable antenna reflectors. Large Deployable Antenna Workshop, 2–3 October 2012, ESA-ESTEC, Noordwijk, The Netherlands
 57. Salama, M., Jenkins, C.H.: Intelligent gossamer structures: a review of recent developments and future trends. AIAA paper 2001-1196 (2001)
 58. Thomson, M.: The Astromesh deployable reflector. In: Proceedings of Antennas and Propagation International Symposium (1999). doi:[10.1109/APS.1979.838231](https://doi.org/10.1109/APS.1979.838231) Israel
 59. TecSar: Encyclopedia Astronautica. <http://www.astronautix.com/craft/tecsar.htm>
 60. Wade, W.D.: Development of low PIM, zero CTE mesh for deployable communication antennas. In: Proceedings of MIL-COM 90 Conference, pp. 1175–1178 (1990)
 61. Miura, A., Tanaka, M.: A mesh reflecting surface with electrical characteristics independent on direction of incident wave. In: Proceedings of Antennas and Propagation Symposium 2004. doi:[10.1109/APS.2004.1329546](https://doi.org/10.1109/APS.2004.1329546)
 62. Di, J., Duan, B., Zheng, F.: Reflector shape adjusting methods for cable mesh deployable antennas. In: 1st International Symposium on Systems and Control in Aerospace and Astronautics (2006). doi:[10.1109/ISSCAA.2006.1627522](https://doi.org/10.1109/ISSCAA.2006.1627522)
 63. Datashvili, L., Baier, H., Wehrle, E., Kuhn, T., Hoffmann, J.: Large shell-membrane space reflectors. In: Proceedings of AIAA Structures, Dynamics, and Materials Conference, Honolulu, Hawaii (2010)
 64. Datashvili, L., Baier, H.: Flexible fiber composites for space structures. In: Chang, G. (ed.) *Fiber Composite Structures*. Nova Science Publishers, Inc., USA (2011)
 65. Schmid, M., Barho, R.: Development of an Unfurlable CFRP skin reflector. In: Proceedings of 25th Antenna Workshop, ESTEC, Noordwijk (2002)
 66. Devilliers, C., Kroedel, M.: CESIC—optomechanical developments for space mirrors. In: 7th International Conference on Space Optics, October 2008
 67. Sein, E., Toulemont, Y., Safa, F., Duran, M., Deny, P., De Chambure, D., Passvogel, T., Pilbratt, G.: A 3.5 M SiC Telescope for HERSCHEL mission. In: Conference Proceedings Space Telescopes and Instruments, SPIE 4850 (2003)
 68. Flint, E., Lindler, J., Hall, J., Rankine, C., Regelbrugge, M.: Overview of form stiffened thin film shell characteristic behavior. In: 47th AIAA/ASME/ASCE/AHS/ASC Structures, Structural Dynamics, and Materials Conference (2006). doi:[10.2514/6.2006-1900](https://doi.org/10.2514/6.2006-1900)
 69. Pearson, J.C., Unroe, M.R.: Precision Tooling for Thin Film Membrane Reflectors. *AMPTIAC Q.* **8**(1) (2004)
 70. Jenkins, C.H., Tampi, M., Kalanovic, V.D., Padmanabhan, K.: Practical aspects of precision membrane antenna shape control. In: IEEE International Conference on Systems, Man and Cybernetics (1998). doi:[10.1109/ICSMC.1998.726494](https://doi.org/10.1109/ICSMC.1998.726494)
 71. Andersen, G.: Large optical photon sieve. *Opt. Lett.* **30**(22) (2005)
 72. Baier, H., Datashvili, L., Ender, S., Roose, S., Rodrigues, G.: Large deployable telescopes—also for μm -wavelengths? In: Proceedings of ESA Large Deployable Antenna Workshop, Noordwijk, October 2012
 73. Rapp, S., Baier, H.: Shape memory polymer actuator patches for shape adjustment of fiber composite parts. In: Proceedings of 19th AIAA/ASME/AHS Adaptive Structures Conference, Denver, USA, 2011
 74. Leng, J., Du, S.: *Shape Memory Polymers and Multifunctional Composites*. CRC Press, New York (2010)
 75. Bar-Cohen, Y., Leary, S.: Electroactive polymer characterization methods. In: Proceedings of SPIE Symposium Smart Structures and Materials, Newport (2000)
 76. Nella, J., Atcheson, P., Atkinson, C., Au, D., Blair, M., Brownwicki, A., Fitzgerald, D., Heideng, J., Lightsey, P., Kelly, T., Matthews, G., Pohner, J., Reynolds, P., Shuckstes, D., Texter, S.,

- Waldie, D., and Whitley, R.: Next Generation Space Telescope (NGST) observatory architecture and performance. In: Proceedings of the 50th AIAA/ASME/ASCE/AHS/ASC Structures, Structural Dynamics and Materials Conference (2009)
77. Denoyer, K.K., Flint, E.M., Main, J.A., Lindler, J.E.: Actively controlled thin-shell space optics, smart structures and materials. In: Proceedings of SPIE, San Diego, CA, vol. 5054, pp. 263–274 (2003)
78. Dargaville, T.R., Celina, M.C., Elliott, J.M., Chaplya, P.M., Jones, G.D., Mowery, D.M., Assink, R.A., Clough, R.L., Martin, J.W.: Characterization, Performance and Optimization of PVDF as a Piezoelectric Film for Advanced Space Mirror Concepts. Report No. SAND2005-6846, Sandia National Laboratories, 2005
79. Rodrigues, G., Bastaitis, R., Roose, S., Stockman, Y., Gebhardt, S., Schoenecker, A., Villon, P., Preumont, A.: Large lightweight segmented mirrors for adaptive optics. In: Proceedings SPIE Conference on Astronomical Instrumentation—Adaptive Optics Systems (7015), Marseille, France, June 23–28, 2008
80. Fang, H., Pattom, M., Wang, K., Im, E.: Shape control of large membrane reflectors with PVDF actuation. In: AIAA Structures, Dynamics and Materials Conference, Honolulu, Hawaii, AIAA paper 2077-1842 (2007)
81. Rapp, S., Kang, L., Mueller, U., Han, J.H., Baier, H.: Dynamic shape estimation by modal approach using fiber bragg grating strain sensors. In: SPIE Conference on Smart Structures and Materials 2007—Sensors and Smart Structures Technologies, 18–22. March 2007, San Diego, CA. Proceedings vol. 6529 (2007)
82. Gawronski, W.: Dynamics and Control of Structures—A Modal Approach. Springer, New York (1998)
83. Preumont, A.: Vibration Control of Active Structures—An Introduction, 2nd edn. Kluwer Academic Publishers, Dordrecht (2004)
84. Su, T., Craig, R.: Model reduction and control of flexible structures using Krylov vectors. *J Guid Control Dyn* **14**(2), 260–267 (1991)
85. Antoulas, A.C., Sorensen, D.C.: Approximation of large-scale dynamical systems: an overview. *Int J Appl Math Comput Sci* **11**(5), 1093–1121 (2001)
86. Yoo, E.J., Baier, H.: Parametric model order reduction techniques for simulating active shape and vibration control of the large space structures. In: Proceedings of European Conference on Spacecraft Structures, Materials and Mechanical Testing, Toulouse, September 2009
87. Yoo, E.J.: Parametric Model Order Reduction for Structural Analysis and Control. Doctoral thesis, TU Muenchen (2010) (available via www)
88. Clarricoats, P.J.B., Zhou, H.: Design and performance of a reconfigurable mesh reflector antenna Part 1: Antenna design. Paper 8306H (EI I). In: IEE Proceedings-H, vol. 13X. No. 6, December 1991
89. Pontoppidan, K.: Light-weight reconfigurable reflector antenna dish. In: Proceedings of 28th ESA Antenna Workshop on Space Antenna Systems and Technologies, 31 May–3 June 2005 ESA/ESTEC, Noordwijk, The Netherlands (2005)
90. Datashvili, L., Baier, H., Wei, B., Hoffman, J., Wehrle, E., Schreider, L., Mangenot, C., Santiago-Prowald, J., Scolamiero, L., Angevain, J.-C.: Mechanical investigations of in-space-reconfigurable reflecting surfaces. In: Proceedings of the 32nd ESA Antenna Workshop on Antennas for Space Applications, ESA/ESTEC, Noordwijk, The Netherlands (2010)
91. Datashvili, L., Baier, H., Wei B., Endler, S., Schreider, L.: Design of a morphing skin using flexible fiber composites for space-reconfigurable reflectors. In: AIAA Structures, Dynamics and Materials Conference, Boston, USA (2013)
92. Endler, S., Datashvili, L., Baier, H., Schreider, L.: Nano-fillers in fiber reinforced polymers for performance enhancement of satellite structures. In: Proceedings of the ESA Structures Conference, Noordwijk, The Netherlands, March 2012
93. Washington, G., Yoon, H.-S., Angelino, M., Theunissen, W.H.: Design, modelling, and optimization of mechanically reconfigurable aperture antennas. *IEEE Trans Antennas Propag* **50**, 628–637 (2002)
94. Rodrigues, G., Angevain, J.C., Santiago-Prowald, J.: Shape optimization of reconfigurable antenna reflectors. In: Proceedings of ESA Workshop on Large Deployable Antennas, ESTEC, Noordwijk, October 2012